

THE TURBULENT JET FROM A SERIES OF
HOLES IN LINE

by

R. Knystautas

Thesis submitted in partial fulfillment
of the requirements for the degree of
Master of Engineering

Department of Mechanical Engineering

McGill University

Montreal

April 1962

SUMMARY

The possibility of obtaining two-dimensional turbulent jet flow from a series of closely-spaced uniform holes in line has been investigated both theoretically and experimentally. The case studied was that of a jet discharging into still fluid of similar density at incompressible speeds. Such a quasi two-dimensional jet is a particular example of a multiple-interfering jet group.

Reichardt's hypothesis for the turbulent shear stress in a free jet linearizes the equation of motion for the mean square downstream velocity and thus enables the superposition of this parameter for multiple-interfering jets. As a result, the start of the two-dimensional flow and the location of the hypothetical origin of the quasi two-dimensional jet may be predicted. At sufficiently large Reynolds Numbers, these positions, expressed non-dimensionally in terms of hole diameter, are a function of the non-dimensional hole spacing only. Fully merged two-dimensional flow occurs at approximately twelve hole spacings downstream of the exit plane and the downstream momentum remains effectively constant. The hypothetical origin is generally located a short distance downstream of the exit plane provided that the hole spacing-to-diameter ratio is greater than one. The

theoretical predictions agree reasonably well with experiment even to the extent of predicting the mean velocity profiles before two-dimensionality is reached.

A brief experimental investigation has also been made of the Coanda deflection of the quasi two-dimensional jet by adjacent boundaries. The quasi two-dimensional jet separates from an adjacent circular cylinder at a somewhat smaller angular distance than does an equivalent two-dimensional jet. Surprisingly, the quasi two-dimensional jet readily reattaches to an inclined flat plate although it does so further downstream for each plate inclination than does its two-dimensional counterpart.

ACKNOWLEDGEMENTS

The author is deeply indebted to Dr. B.G. Newman for his guidance and advice throughout the course of this work.

The numerous suggestions and valuable help given by the workshop technical staff, in particular Messrs. A. Gustavsen and E. Hansen, during the construction of the apparatus is very much appreciated.

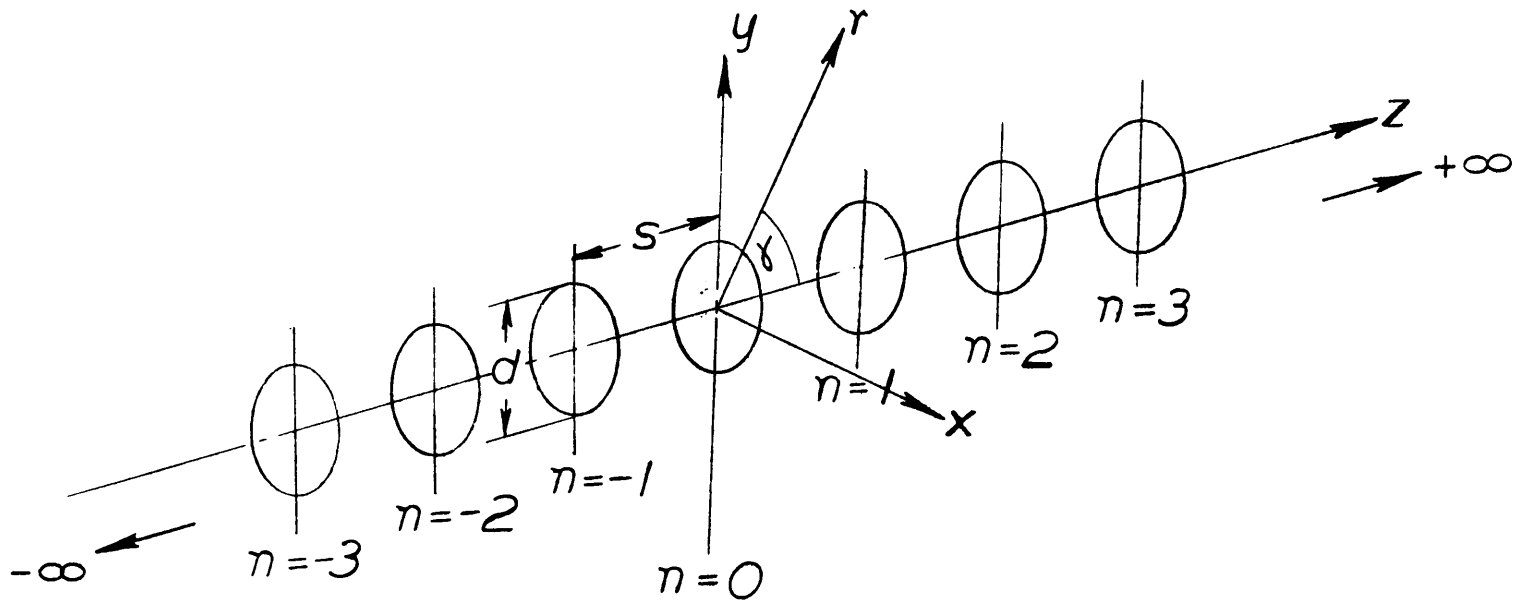
Thanks are due to Miss J. MacPherson of the McGill Computing Center for her help in programming, on the IBM 650 Computer, some of the theoretical problems encountered throughout the work.

The work was supported by the Defence Research Board of Canada under DRB Grant No. 9551-12.

CONTENTS

	Page
SUMMARY	i
ACKNOWLEDGEMENTS	iii
CONTENTS	iv
NOTATION	v
1. INTRODUCTION	1
2. DIMENSIONAL ANALYSIS	6
3. THEORETICAL ANALYSIS	9
4. DETAILS OF THE EXPERIMENTAL INVESTIGATION	17
5. DISCUSSION OF EXPERIMENTAL RESULTS AND COMPARISON WITH THEORY	19
5.1 The Two-Dimensional Jet Discharging Freely	19
5.2 The Quasi Two-Dimensional Jet Discharging Freely	21
5.3 The Deflection of the Quasi Two- Dimensional Jet by Adjacent Boundaries ..	25
6. CONCLUSIONS	28
APPENDIX	30
REFERENCES	36

NOTATION



- a radius of circular cylinder for Coanda deflection
- A_0 discharge area of a single hole
- b slot width or the width of the free jet as in Equation 9
- b_e discharge area per unit span or equivalent two-dimensional slot width
- c constant of proportionality in Equation 27
- C_m constant of proportionality in Equation 12
- d hole diameter
- e base of the natural logarithm
- f 'function of'
- J downstream momentum obtained by numerical integration of mean velocity profiles
- J' jet momentum efflux per unit span, neglecting the internal boundary layers ($=2(p_0 - p_\infty)b_e$)
- J_0 momentum efflux in the plane of the flow discharge
- K_0 constant as in Equation 11

- ℓ length of inclined flat plate for Coanda deflection
- n numbered order of jets from the origin at $n=0$,
as in the above figure
- p static pressure
- p_0 supply pressure
- p_s static pressure on the surface of the face-block
- p_∞ pressure of the still surroundings
- p_ϕ pressure measured by the round Pitot tube during
pitch and yaw calibration
- r, γ, x cylindrical polar coordinates with the origin at
 $n = 0$
- R_e Reynolds Number
- s distance between adjacent holes
- u mean velocity in the longitudinal direction x
- u_c maximum mean longitudinal velocity in the jet
at any x
- u_m minimum mean longitudinal velocity in the center-
plane $y = 0$ at any x in the jet
- u_0 discharge velocity $(= \sqrt{\frac{2}{\rho} (p_0 - p_\infty)})$
- u' turbulent fluctuating component of velocity in
the longitudinal direction x
- U instantaneous velocity in the longitudinal
direction x
- V instantaneous velocity in the transverse direction r
- x, y, z Cartesian coordinates with origin at $n = 0$, as
shown in the above figure
- x_0 distance of the hypothetical origin from the
discharge plane

- x_{2D} identifies the start of the two-dimensional region of the quasi two-dimensional jet
- x_R distance of the reattachment point from the discharge plane for the inclined plate
- X transformed variable replacing the time variable in the two-dimensional diffusion equation
($= C_m^2 x^2 / 4$)
- $y_c/2$ value of y for which $u = \frac{u_c}{2}$
- α angle between the inclined plate and the axis of the undeflected jet
- ρ density of both the emerging and the surrounding fluid
- ν kinematic viscosity
- Λ momentum transfer length, defined in Equation 9
- θ angular position on the surface of the circular cylinder
- θ_{sep} angular position of separation on the circular cylinder
- σ constant as in Equation 28
- ϕ pitch or yaw angle of the Pitot tube during calibration
- ϵ amplitude of undulating mean velocity profile, as defined by Equation 23
- ∇ vector operator, del

1. INTRODUCTION

The fluid flow emanating from a series of closely-spaced uniform holes in line has been studied both experimentally and theoretically to determine whether or not it tends to become effectively two-dimensional downstream. The case considered is that when the surrounding fluid is of similar density and at rest. The Coanda deflection of such a quasi two-dimensional jet by adjacent boundaries has also been studied experimentally in a similar fashion to the two situations examined by Bourque and Newman⁽²⁾, (7) for a two-dimensional jet. The speeds involved were sufficiently low for the flow to be effectively incompressible.

The quasi two-dimensional jet may be used for jet-flapped wings⁽⁸⁾, thrust augmentors, and generally in the field of boundary layer control by blowing. For such applications it is structurally preferable to emit the jet from a series of holes rather than from a continuous uniform slot and it may be desirable to attain two-dimensionality at a reasonable distance downstream without too great a loss in the velocity of the merged flow. As a result, emphasis is placed on predicting the distance downstream of the jet exit at which the flow becomes effectively two-dimensional, that is, where the merging axisymmetric jets lose their individual identities and behave as a single two-dimensional jet.

The quasi two-dimensional jet is a particular example of a multiple-interfering jet group and a theoretical study of such jet groups is, in general, difficult. Even the simplest classical two-dimensional and axisymmetric jets have not been completely analysed although they have been investigated quite extensively in the light of the available hypotheses for free turbulent flow. Thus, some knowledge of their behavior is available and an attempt can be made to study the multiple-interfering jets in terms of the two simpler cases.

Tollmien⁽¹³⁾ attempted the initial theoretical treatment of both the two-dimensional and the axisymmetric jets on the basis of Prandtl's mixing length hypothesis⁽¹²⁾. Görtler⁽⁴⁾ carried out a somewhat simpler treatment using Prandtl's modification of Boussinesq's concept for a turbulent eddy viscosity. Prandtl assumed that the eddy viscosity is constant across the flow at each downstream position and thus is proportional to the product of the maximum velocity and the width of the jet there.

In the foregoing analyses the flow is assumed to originate with a certain momentum from an infinitesimal slot or hole. The analyses are applicable to the flow from a finite slot or hole sufficiently far downstream when a suitable hypothetical origin is chosen. This origin is the position of the infinitesimal slot or hole from which flow with the same momentum would produce

the same velocity profiles far downstream. In practice, the flow emerges as a uniform laminar jet and mixes with the surroundings so that the width of the central core of uniform velocity gradually diminishes. The jet becomes fully mixed and turbulent only a certain number of diameters or slot widths downstream of the exit⁽¹⁴⁾.

It is mathematically difficult to extend the mixing length theories to complex situations involving multiple-interfering jet groups. However, the inductive theory of free turbulence introduced by Reichardt⁽⁹⁾ may be extended to such cases because the equation of motion in the downstream direction is linearized⁽¹⁾. This theory is based on a critical examination of experimental results for free turbulent flow in which it was noted that the experimental data for mean velocity are well represented by an error function.

In all the above theories, it is assumed that both the variations in the static pressure across the jet and the longitudinal normal stresses are negligible compared with the central dynamic pressure and thus the mean jet momentum is conserved. Miller and Comings⁽⁵⁾, by means of meticulous experimental investigation, showed that the variations in static pressure across a two-dimensional jet are of the same order of magnitude as the variations of the normal turbulent stresses, but of opposite sign. As a result, there exists a near-

cancellation of these variations in the region of turbulence even though the individual magnitudes are significant.

There is relatively little information available on multiple-interfering free jets. Miller and Comings⁽⁶⁾ investigated experimentally the flow from two parallel, two-dimensional air jets mixing in otherwise still air. Entrainment in the confined region between the jets produces pronounced negative pressures there. This effect causes the jet streamlines to be deflected inwards so that the flows merge with backflow at the point of meeting and the establishment of two counter-rotating vortices in the confined region. On the average, the flow is symmetrical about the centerplane and the conditions on one side resemble those for a jet issuing parallel to an offset from a flat plate for which theories are given by Bourque and Newman⁽²⁾ and by Sawyer⁽¹⁰⁾. Another consequence of the negative pressure in the confined region is that the momentum of the merged flow is less than the combined momentum of the flow emerging from the two slots. Downstream, the merged jets lose their individual identities and behave as a single two-dimensional jet with subsequent conservation of the remaining momentum.

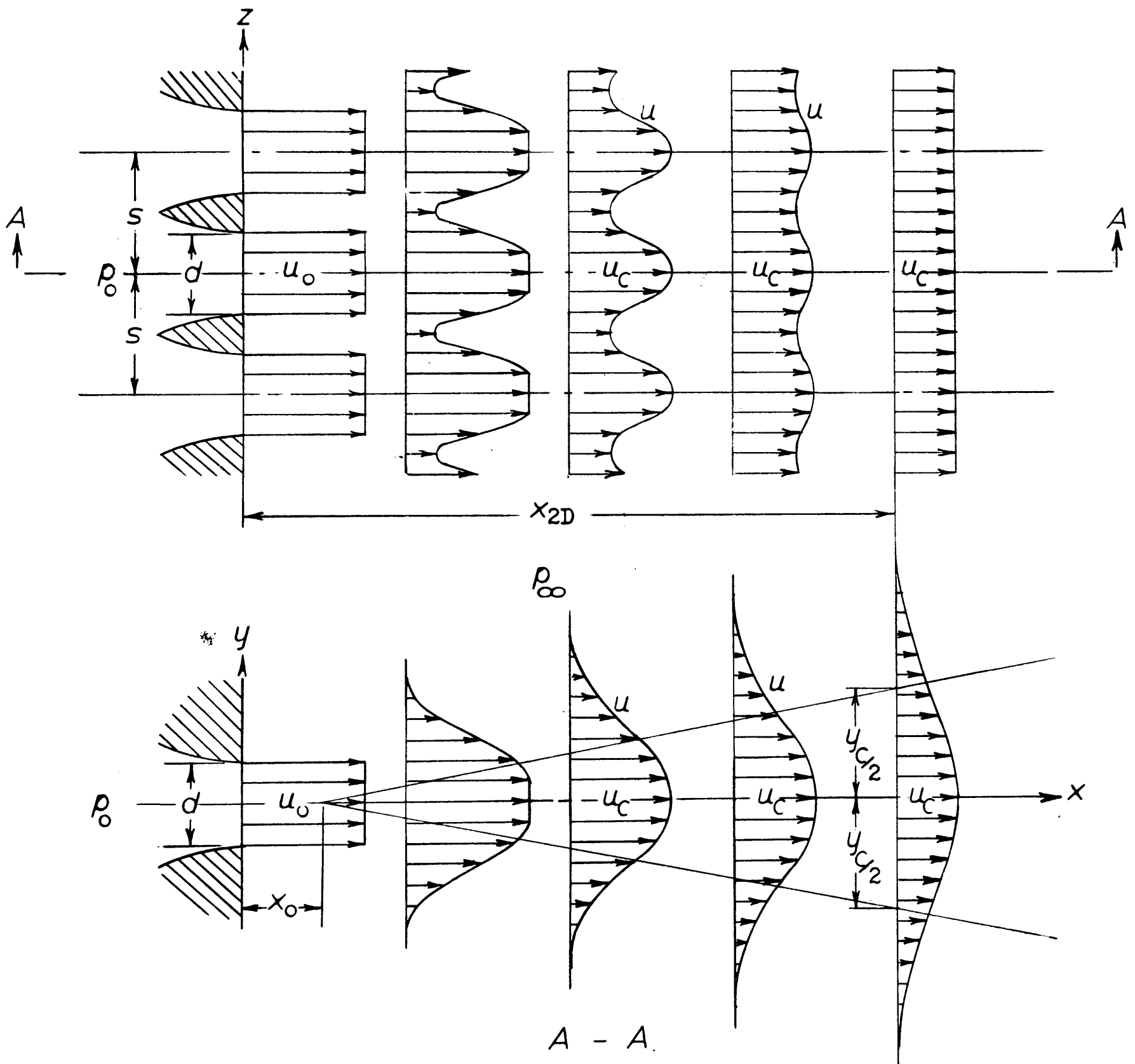
Alexander, Baron and Comings⁽¹⁾ have investigated the mixing of two parallel axisymmetric air jets discharging into still air. Predictions on the basis of Reichardt's inductive theory are in fair

agreement with their measurements of the distribution of downstream momentum flux. The flow round the jets is now vented to the surroundings so that the jets are only slightly deflected toward one another and the downstream momentum is very nearly equal to that emerging from the holes.

In the present investigation, Reichardt's inductive theory is used in the analysis to predict the start of the two-dimensional region and the location of the hypothetical origin of the quasi two-dimensional jet. The theoretical predictions are compared with experimental measurements for three values of hole spacing. Brief studies of the Coanda deflection of the quasi two-dimensional jet by adjacent boundaries were also undertaken and are compared with the measurements of a similarly deflected two-dimensional jet made by Bourque and Newman^{(2),(7)}. A circular cylinder and an inclined flat plate were used as the jet deflecting boundaries.

2. DIMENSIONAL ANALYSIS

The flow in the quasi two-dimensional jet is illustrated in Figure 1. It is assumed to be effectively incompressible.



A - A.

FIG. 1

The relevant parameters which suffice to define the flow are

- $p_0 - p_\infty$ the supply pressure relative to the surroundings
- ρ the fluid density
- ν the kinematic fluid viscosity
- d the diameter of the discharge holes
- s the distance between adjacent holes

The relevant non-dimensional criteria of similarity may be written as

$$\frac{s}{d}, \left[\frac{(p_0 - p_\infty) d^2}{\rho \nu^2} \right]^{1/2}$$

The downstream distance x_{2D} of the point where the flow becomes effectively two-dimensional can be expressed in terms of these non-dimensional criteria as

$$\frac{x_{2D}}{d} = f \left\{ \frac{s}{d}, \left[\frac{(p_0 - p_\infty) d^2}{\rho \nu^2} \right]^{1/2} \right\} \dots\dots (1)$$

Similarly, the location x_0 of the hypothetical origin of this merged two-dimensional flow can be expressed as

$$\frac{x_0}{d} = f \left\{ \frac{s}{d}, \left[\frac{(p_0 - p_\infty) d^2}{\rho \nu^2} \right]^{1/2} \right\} \dots\dots (2)$$

For sufficiently high Reynolds Numbers transition in the mixing layers occurs close to the slot and the effect of variations in fluid viscosity in the subsequent turbulent flow can be assumed to be confined to the

smallest eddies. The mean flow or the structure of the large scale eddies can be assumed to be insensitive to these variations, that is, insensitive to changes in Reynolds Number⁽¹⁴⁾. In view of this simplification

$$\frac{x_{2D}}{d} = f\left(\frac{s}{d}\right) \quad \dots (3)$$

$$\frac{x_0}{d} = f\left(\frac{s}{d}\right) \quad \dots (4)$$

3. THEORETICAL ANALYSIS

The momentum equation for the time-averages of velocity for incompressible turbulent flow in a single axisymmetric jet discharging freely can be written in cylindrical coordinates as

$$\frac{\partial}{\partial x} \left(\frac{p}{\rho} + \overline{U^2} \right) + \frac{1}{r} \frac{\partial}{\partial r} (r\overline{UV}) = 0 \quad \dots (5)$$

where U and V are the instantaneous velocities in the directions x and r

p is the static pressure

and the Reynolds Number is assumed to be sufficiently high for the viscous terms to be unimportant.

The effect of variations in the downstream static pressure may be neglected in the light of the conclusions drawn by Miller and Comings⁽⁵⁾ for the two-dimensional jet if $\overline{U^2}$ were replaced by the square of the mean velocity u^2 . However, $\frac{\overline{u'^2}}{u^2}$ is generally small (1-2%) so that within the accuracy of the present theory it is justifiable to neglect the effects of the longitudinal fluctuating component $u' = U - u$.

Since the pressure is everywhere ambient

$$\int_0^\infty \rho u^2 2\pi r dr = \text{the jet momentum, } J \quad \dots (6)$$

and equation (5) can be rewritten

$$\frac{\partial u^2}{\partial x} + \frac{1}{r} \frac{\partial}{\partial r} (r\overline{UV}) = 0 \quad \dots (7)$$

On the basis of Reichardt's inductive theory of free turbulence

$$\overline{UV} = -\Lambda \frac{\partial \overline{U^2}}{\partial r} \dots\dots (8)$$

where

$$\Lambda = \frac{b}{2} \frac{db}{dx} \dots\dots (9)$$

and b is a function of x only.

Equation (7) can be rearranged as

$$\frac{\partial u^2}{\partial x} - \frac{b}{2r} \frac{db}{dx} \frac{\partial}{\partial r} \left(r \frac{\partial u^2}{\partial r} \right) = 0 \dots\dots (10)$$

and solved to give

$$u^2 = \frac{K_0}{b^2} e^{-(r/b)^2} \dots\dots (11)$$

From equations (6) and (11) it is clear that

$$b \propto x$$

or $b = C_m x \dots\dots (12)$

and that $K_0 = \frac{J}{\pi \rho}$

or $K_0 = \frac{u_0^2 A_0}{\pi} \dots\dots (13)$

since $J = \rho u_0^2 A_0$ for an axisymmetric jet,

Equation (11) can be rewritten as

$$\frac{u^2}{u_0^2} = \frac{A_0}{\pi C_m^2 x^2} e^{-(r/C_m x)^2} \dots\dots (14)$$

Equation (10) can be rearranged with the aid of equation (12) to give

$$\frac{\partial u^2}{\partial x} - \frac{C_m^2 x}{2r} \frac{\partial}{\partial r} \left(r \frac{\partial u^2}{\partial r} \right) = 0 \quad \dots (15)$$

By putting $C_m^2 x^2 = 4X$ gives

$$\frac{\partial u^2}{\partial X} - \frac{1}{r} \frac{\partial}{\partial r} \left(r \frac{\partial u^2}{\partial r} \right) = 0 \quad \dots (16)$$

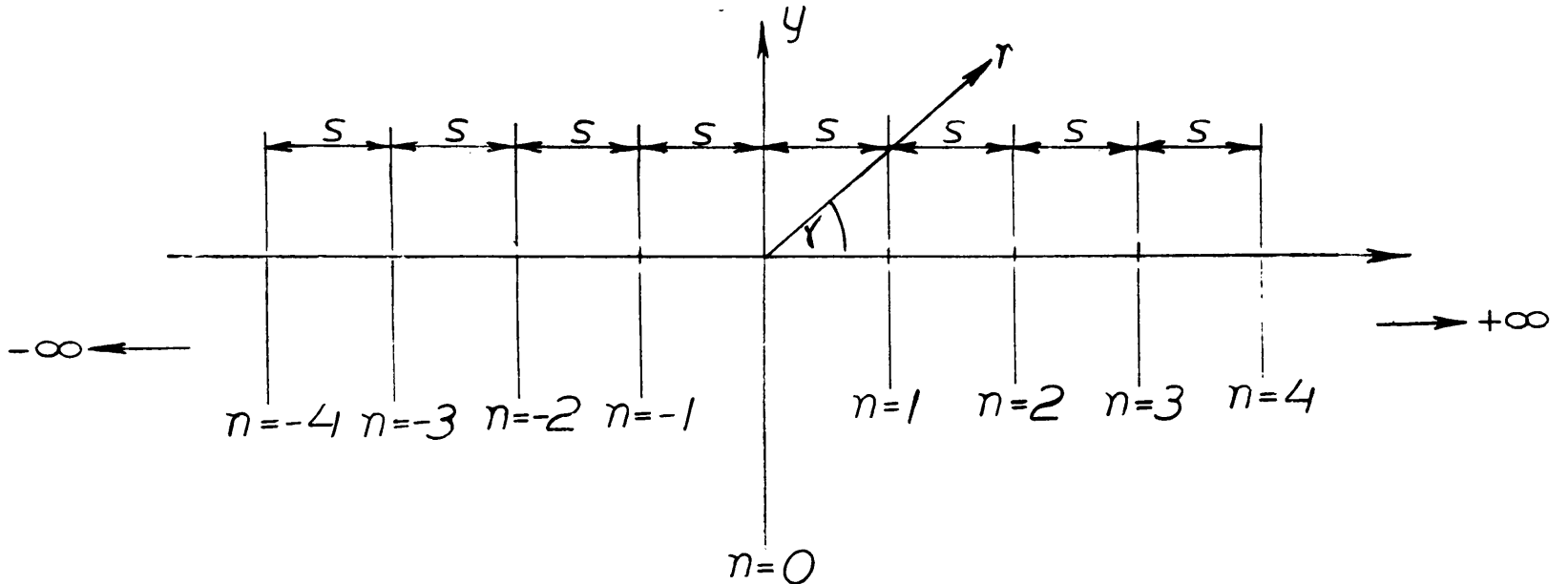
Equation (16) is the two-dimensional diffusion equation

$$\nabla^2(u^2) = \frac{\partial u^2}{\partial X}$$

where X is positive and replaces the time variable.

As noted by Alexander, Baron and Comings⁽¹⁾, equation (15) is then a linear partial differential equation whose solution for the axisymmetric jet is given by equation (14). It is invariant to the position of the origin and the orientation of the axes y and z . Equation (14) represents the momentum flux within an axisymmetric jet with hypothetical origin at $x=0$. The summation of individual particular solutions of a linear and invariant differential equation is itself a solution and this important result permits an extension of the theory to the quasi two-dimensional jet. The momentum flux at any point in the quasi two-dimensional jet can be considered as the net summation of the momentum flux contributions from individual axisymmetric jets spaced at a distance s apart. The central jet can be considered

to emanate from the origin of a cylindrical coordinate system (r, γ, x) and the others to extend symmetrically in both directions along the z axis.



In terms of the coordinate system (r, γ, x) and the numbered order n of the holes from the origin, the square of the mean velocity in the quasi two-dimensional jet can be expressed mathematically as follows:

$$\frac{u^2}{u_0^2} = \frac{A_0}{\pi C_m^2 x^2} \sum_{n=-\infty}^{+\infty} e^{-\left[\frac{r^2 + (ns)^2 - 2rns \cos \gamma}{C_m^2 x^2} \right]} \quad \dots (17)$$

On the centerplane $y = 0$ this becomes

$$\left[\frac{u^2}{u_0^2} \right]_{y=0} = \frac{A_0}{\pi C_m^2 x^2} \sum_{n=-\infty}^{+\infty} e^{-\left[\frac{r-ns}{C_m x} \right]^2} \quad \dots (18)$$

$$\frac{u_c^2}{u_0^2} = \frac{A_0}{\pi C_m^2 x^2} \sum_{n=-\infty}^{+\infty} e^{-\left[\frac{ns}{C_m x} \right]^2} \quad \dots (19)$$

$$\frac{u_m^2}{u_0^2} = \frac{A_0}{\pi C_m^2 x^2} \sum_{n=-\infty}^{+\infty} e^{-\left[\left(\frac{2n-1}{2} \right) \frac{s}{C_m x} \right]^2} \quad \dots (20)$$

$$\frac{u_c^2}{u_0^2} - \frac{u_m^2}{u_0^2} = \frac{A_0}{\pi C_m^2 x^2} \sum_{n=-\infty}^{+\infty} \left\{ e^{-\left[\frac{ns}{C_m x} \right]^2} - e^{-\left[\left(\frac{2n-1}{2} \right) \frac{s}{C_m x} \right]^2} \right\} \quad \dots (21)$$

Examination of equation (21) reveals that it is a measure of the amplitude of the undulating mean velocity profile in the plane $y = 0$. A minimum amplitude ϵ can be prescribed at which the undulation could be considered as having effectively vanished. This can be taken as the start of the fully merged two-dimensional flow whose downstream location can be designated by x_{2D} .

Mathematically,

$$x_{2D} \stackrel{\equiv}{=} x_{\min} \quad \text{for which}$$

$$\frac{u_c^2}{u_o^2} - \frac{u_m^2}{u_o^2} = \epsilon, \quad \text{say} \quad \dots (22)$$

With $A_o = \frac{\pi d^2}{4}$, equations (21) and (22)

can be combined and rearranged as

$$\frac{1}{4C_m^2 \left(\frac{x_{2D}}{d}\right)^2} \sum_{n=-\infty}^{+\infty} \left\{ e^{-\left[\frac{n}{C_m} \cdot \frac{s}{x_{2D}}\right]^2} - e^{-\left[\frac{(2n-1)}{2C_m} \cdot \frac{s}{x_{2D}}\right]^2} \right\} = \epsilon$$

..... (23)

Equation (23) is an implicit relation for x_{2D} in terms of the non-dimensional hole spacing $\frac{s}{d}$, and enables the functional relationship in equation (3) to be determined. Equation (23) involves the experimental evaluation of a single arbitrary constant C_m . Based on experiments performed using a single axisymmetric jet, a mean value of $C_m = 0.077$ was obtained (Figure 2), which agrees reasonably well with the value of $C_m = 0.075$ obtained by Alexander et al⁽¹⁾. Furthermore the measurements shown in Figure 3 indicate that x_o is

effectively zero for a single axisymmetric jet as has been implicitly assumed in the above theory. Although the relation for x_{2D} given in equation (23) is implicit, it is of interest to note that the series converges very rapidly and **that** the evaluation of the first few terms generally suffices. Equation (23) can be readily solved using a minimization routine on a digital computer as was done in the present investigation.

Beyond $x = x_{2D}$, the effectively two-dimensional flow can be thought of as having originated from an infinitesimal hypothetical slot. For such a case, equation (19) can be rewritten in integral form as

$$\frac{u_c^2}{u_o^2} = \frac{b_e}{\pi C_m^2 x^2} \int_{-\infty}^{\infty} e^{-\left(\frac{z}{C_m x}\right)^2} dz \quad \dots (24)$$

since it can be considered that $s \rightarrow dz$ and $ns \rightarrow z$ for the infinitesimal hypothetical slot, and that

$$\rho u_o^2 A_o = \rho u_o^2 b_e s = J$$

where, since momentum is conserved, b_e is the area of the holes per unit span for the quasi two-dimensional jet, so that

$$J' = \rho u_o^2 b_e \quad \dots (25)$$

Equation (24) can be simplified to give

$$\frac{u_c^2}{u_o^2} = \frac{b_e}{\sqrt{\pi} C_m x} \quad \dots (26)$$

For the two-dimensional jet

$$u_c^2 \propto \frac{1}{x - x_0}$$

or

$$\frac{u_c^2}{u_0^2} = \frac{c}{x - x_0} \quad \dots\dots (27)$$

According to Newman(7)

$$c = \frac{3}{4} \sigma b, \quad \text{where } \sigma = 7.7 \quad \dots\dots (28)$$

On the basis of equation (26) and

$$C_m = 0.077$$

$$x_0 = 0 \quad \text{and} \quad \sigma = 9.75$$

Although equation (26) does not give a good prediction for the location x_0 of the hypothetical origin of the quasi two-dimensional jet, it is significant in the sense that it gives a theoretical value for σ based on measurements in an axisymmetric jet which is similar to that obtained experimentally for a two-dimensional jet. Thus, the constants determining the rate of growth of a two-dimensional and an axisymmetric jet have been related.

An alternate expression for x_0 can be obtained by recalling that for $x = x_{2D}$, the flow is effectively two-dimensional and behaves in accordance with the laws for two-dimensional jet flow.

In particular, from equation (27)

$$\left[\frac{u_c^2}{u_0^2} \right]_{x=x_{2D}} = \frac{c}{x_{2D} - x_0}$$

from which

$$x_o = x_{2D} - c \left[\frac{u_o^2}{u_c^2} \right]_{x=x_{2D}} \dots (29)$$

Using Newman's result, as in equation (28)

$$\frac{x_o}{d} = \frac{x_{2D}}{d} - 5.775 \frac{b_e}{d} \left[\frac{u_o^2}{u_c^2} \right]_{x=x_{2D}}$$

Thus using equation (26)

$$\frac{x_o}{d} = \frac{x_{2D}}{d} - 5.775 \frac{b_e}{d} \sqrt{\pi} \frac{C_m}{b_e} x_{2D}$$

$$\frac{x_o}{d} = 0.212 \frac{x_{2D}}{d} \dots (30)$$

4. DETAILS OF THE EXPERIMENTAL INVESTIGATION

A detailed description of the experimental apparatus used in the study of the free and the deflected quasi two-dimensional jet is given in the Appendix. A comprehensive experimental study of the quasi two-dimensional jet was made to check the theoretical predictions for the start of the effectively two-dimensional flow and the location of its hypothetical origin. Emphasis was placed on determining the effect of changing the hole spacing in order to verify the predictions of the dimensional analysis and equations (23), (26), and (30).

Velocity profiles in the centerplanes $y = 0$ and $z = 0$ were measured at stations as far downstream as $\frac{x}{d} = 80$ to determine the jet growth laws and to evaluate, by numerical integration using Simpson's rule, the downstream momentum at particular stations. Velocities were determined from pitot tube measurements assuming ambient static pressure everywhere. The extremely good repeatability of the measurements from hole to hole is worthy of note. Static pressures on the face of the plane containing the discharge holes were measured to determine the magnitude of the reduction in pressure associated with entrainment. All observations for the quasi two-dimensional jet were made at three hole spacings with $\frac{s}{d} = 1.5, 2.0, \text{ and } 3.0$ for a range of Reynolds Number $Re = \left[\frac{(p_0 - p_\infty)d^2}{\rho \nu^2} \right]^{1/2}$ between 2.92×10^5

and 2.53×10^6 . Three slot widths with $b = 0.245, 0.188,$ and 0.123 in., were used to study the flow in a two-dimensional jet. A knowledge of the behavior of the latter is required as a basis of comparison for the quasi two-dimensional jet and the measurements were undertaken to verify existing theories for the two-dimensional jet. Downstream mean velocity profiles in a single axisymmetric jet were also measured to determine its rate of growth and the location of the hypothetical origin.

The Coanda deflection of the quasi two-dimensional jet by a circular cylinder and an inclined flat plate was also briefly investigated at a hole spacing $\frac{s}{d} = 1.5$. Measurements of the angular position of separation and the velocity profile near separation are presented for the circular cylinder. Values of the reattachment distance x_R at various angles of plate inclination α are also presented.

All measurements were made at incompressible speeds with $\frac{p_0}{p} > 1.05$.

5. DISCUSSION OF EXPERIMENTAL RESULTS AND COMPARISON WITH THEORY

5.1 The Two-Dimensional Jet Discharging Freely

The flow in a two-dimensional jet was studied at three slot widths with $b = 0.245, 0.188$ and 0.123 in. for a range of Reynolds Number $Re = \left[\frac{(p_0 - p_\infty) b^2}{\rho v^2} \right]^{1/2}$ between 2.0×10^4 and 1.2×10^6 to verify the previous determinations of the location of the hypothetical origin and the jet growth. The flow was satisfactorily two-dimensional (Figure 4) and this is attributed to the uniformity of the supply pressure along the span, the sharpness of the slot lips (absence of Coanda effect) and to the close tolerance (± 0.001 in.) on the width of the slot.

It is well established that for a two-dimensional jet the inverse square of the mean centerline velocity decays in proportion to the downstream distance. In Figure 5, the plot of the inverse square of the mean centerline velocity, expressed non-dimensionally as $\frac{1}{u_c^2} \frac{u_0^2}{u_0^2}$, against the downstream distance $\frac{x}{b}$ gives a universally linear curve for the three slot widths considered. The universal curve has a slope of 0.1722 and compares well with the conventional slope 0.1730 (Equations 27 and 28). A universal hypothetical origin is also obtained whose location $\frac{x_0}{b}$ is the point at which the centerline mean velocity hypothetically approaches infinity as the slot width becomes infinitesimally thin but where $\lim_{b \rightarrow 0} \frac{L t}{b} \rho u_c^2 b = J$ as explained by Newman⁽⁷⁾. The

value of $\frac{x_0}{b}$ is approximately - 1.0.

Similarity of downstream velocity profiles is a well accepted property of the two-dimensional jet (Figure 6) and the jet expands linearly (Figures 7 and 8). The linearity of growth can be evidenced by choosing a point $y_c/2$ in the downstream mean velocity profiles as the value of y where $u = \frac{u_c}{2}$. Extrapolation of this straight line $\frac{y_c}{x}/2$ to $y_c/2 = 0$ gives more accurately an average value $\frac{x_0}{b} = -1.5$ which is in fair agreement with the value of $\frac{x_0}{b} = -1.57$ as obtained by Miller and Comings⁽⁵⁾.

The static pressure variations, measured on the face of the exit plane of the slot differ from the surrounding pressure by less than 1/2% of $(p_0 - p_\infty)$ as shown in Figure 9. The downstream momentum was evaluated by numerically integrating, using Simpson's rule, the square of the mean velocity profiles at particular downstream stations. It is seen in Figure 10 that momentum is very nearly conserved and that it is effectively independent of x although it differs from the value emanating from the holes on the assumption that the internal boundary layers are thin. The corrections in the momentum arising from the consideration of the boundary layers and the face static pressure are also given in Figure 10.

5.2 The Quasi Two-Dimensional Jet Discharging Freely

The main interest in the experimental investigation of the free quasi two-dimensional jet is the determination of the parameters $\frac{x_{2D}}{d}$ and $\frac{x_0}{d}$ for various values of hole spacing $\frac{s}{d}$. On the basis of the well-established conclusions for free turbulence, the flow in the quasi two-dimensional jet is assumed to be insensitive to changes in Reynolds Number, provided the latter is large enough for fully turbulent flow to exist a short distance downstream from the exit plane of the holes. Experimentally, this was verified only in a limited sense because the Reynolds Number = $\left[\frac{(p_0 - p_\infty)}{\rho v^2} d^2 \right]^{1/2}$ could only be varied within a narrow range. In all cases investigated, $d = \frac{1}{2}$ in. so that $(p_0 - p_\infty)$ sets an upper limit to the Reynolds Number if the flow is to remain effectively incompressible. There is likewise a lower limit to the Reynolds Number below which the flow in the jet becomes sensitive to external draughts. The flow in the quasi two-dimensional jet was investigated for a range of Reynolds Number between 2.92×10^5 and 2.53×10^6 and within that range it was insensitive to changes in Reynolds Number, (Figures 10, 11).

The downstream mean velocity profiles along the centerplane $y = 0$ of the quasi two-dimensional jet (Figures 12 and 13) provide a means of determining $\frac{x_{2D}}{d}$ for various hole spacings $\frac{s}{d}$. Thus x_{2D} can be

determined as the downstream distance at which the amplitude of the undulating velocity profile has decreased to the point where it can be considered effectively two-dimensional in the centerplane $y = 0$. For two hole spacings with $\frac{s}{d} = 1.5$ and 3.0 experimental mean velocity profiles in the centerplane $y = 0$ (Figures 12 and 13) are compared with their corresponding theoretical counterparts (Figures 14 and 15) which were determined from equation (18). The agreement is fairly reasonable although equation (18) does not predict velocity profiles closer than eight diameters away from the exit plane (Figures 14 and 15). The mean velocity profiles for $\frac{s}{d} = 3.0$ in three dimensions are shown photographically in Figures 16 and 17 at values of $\frac{x}{d} = 6, 10$ and 20 . The dark sections represent the theoretical mean velocity profiles in three dimensions as obtained from equation (17) and the light sections represent the measured experimental mean velocity profiles. The trend towards two-dimensionality is clearly shown.

In the two-dimensional region of the quasi two-dimensional jet, the velocity profiles are similar (Figure 18) and, to the accuracy of the measurements, momentum is conserved (Figure 10) although it differs from the value emanating from the holes when it is assumed that the internal boundary layers are negligibly thin and that the face pressure is ambient. Furthermore the inverse square of the mean centerline

velocity decays in proportion to the downstream distance (Equation 27) as for a two-dimensional jet. In Figures 5 and 11, the inverse squares of the centerplane velocities $\frac{1/u_c^2}{u_o^2}$ and $\frac{1/u_m^2}{u_o^2}$ are plotted against the downstream distance $\frac{x}{d}$ or $\frac{x}{b_e}$, where u_c is the maximum mean longitudinal velocity in the jet at any x and u_m is the minimum mean longitudinal velocity in the centerplane $y = 0$. Thus x_{2D} can be determined as the downstream distance where the two curves blend together and continue on thereafter as a single linear curve. The mean flow beyond the point $x = x_{2D}$ is indistinguishable from that emanating from a two-dimensional slot. Extrapolation of the linear portion of the curve to the point $\frac{1/u_c^2}{u_o^2} \rightarrow 0$ determines the location x_o of the hypothetical origin, as previously explained. The curves of $\frac{1/u_c^2}{u_o^2}$ vs $\frac{x}{d}$ (Figure 11) are used to determine x_{2D} the start of the two-dimensional flow as well as x_o the location of its hypothetical origin at three hole spacings with $\frac{s}{d} = 1.5, 2.0$ and 3.0 . The values of x_{2D} as obtained in this way are plotted in Figure 19, together with those obtained from Figures 12 and 13 and are compared with the predicted values using equation (23) and $\epsilon = \frac{1}{4}, \frac{1}{2}$ and $\frac{3}{4}\%$. A similar plot of the inverse square of the centerplane velocity $\frac{1/u_c^2}{u_o^2}$ against downstream distance $\frac{x}{b_e}$ is also shown in Figure 5 for the three hole spacings mentioned as well as for the three slot widths $b = 0.245, 0.188$ and 0.123 in.

for the two-dimensional jet. It is interesting to note that in Figure 5 the linear portions of the curves for the quasi two-dimensional jet run parallel to the universal linear curve of the two-dimensional jet but displaced from it, the degree of displacement being a function of the hole spacing $\frac{s}{d}$. This displacement of curves can be attributed to a shift in the hypothetical origin of the quasi two-dimensional jet as predicted by equation (30). The experimental values of x_0 for the quasi two-dimensional jet can be obtained from Figures 5 and 11. The flow in the two-dimensional region also expands linearly (Figures 20 and 21) and extrapolation of the straight line $\frac{y_c}{x}/2$ to $y_c/2 = 0$ in Figures 20 and 21 gives a second value for the location x_0 of the hypothetical origin. These values are compared with the theory in Figure 19, and it is interesting to note that they lie between the values given by equation (30) and $x_0 = 0$ as predicted directly from the theory.

The static pressure variations, measured on the face of the exit plane of the holes along a line midway between two holes, are shown in Figure 22. It is noted that they differ from the surrounding pressure by less than 1/2% of $(p_0 - p_\infty)$. This serves to confirm the absence of any pronounced low pressure regions between the holes. The pressure variations, though small on the average, possess certain interesting trends which depend on hole spacing $\frac{s}{d}$ and on the offset

distance y . For example, the static pressure is not least for small y but decreases with increasing y for a certain range and finally increases again gradually to the ambient pressure. This phenomenon may possibly be attributed to the final slowing down of the entrained flow near the jet exit. The variations decrease with increasing $\frac{s}{d}$.

5.3 The Deflection of the Quasi Two-Dimensional Jet by Adjacent Boundaries

The position of angular separation on the circular cylinder of radius $a = 6.5$ in., estimated by means of goose down tufts attached to the surface occurred at $\theta_{sep} = 200^\circ$ at a Reynolds Number $\left[\frac{(p_o - p_\infty)}{\rho v^2} b_e a \right]^{1/2} = 5.5 \times 10^4$ and $\frac{b_e}{a} = 0.04$. The mean velocity profile measured at $\theta = 180^\circ$ is shown in Figure 23 and indicates that the flow is close to separation. The Reynolds Number is defined in this way to provide a basis of comparison with observations made by Newman⁽⁷⁾ on the Coanda deflection of a two-dimensional jet. He found that for $R_e > 4 \times 10^4$ and $\frac{b}{a}$ ranging from 0.02 to 0.04, the angular position of separation $\theta_{sep} = 240^\circ$. It would seem that separation occurs somewhat earlier for the quasi two-dimensional jet than for the two-dimensional jet under similar conditions. Indeed for this particular spacing $\frac{s}{d} = 1.5$, the point of separation more closely corresponds to that for a two-dimensional jet if the diameter d of

the holes is used in place of the equivalent slot width b_e . For this case $\frac{d}{a} = 0.078$ and the point of separation for a two-dimensional jet with the same $\frac{b}{a} = 0.078$ is $\theta = 217^\circ$. It is pertinent to note that when the individual circular jets flow round the cylinder, the reverse curvature at the edge of the jets will cause the flow to merge more slowly.

When the cylinder is replaced by an inclined plate, the flow is still deflected despite the fact that the low pressure near the surface must be increased by the venting to atmosphere between the individual jets. The position of reattachment plotted as $\frac{x_R}{d}$ and as $\frac{x_R}{b_e}$ against the angle of plate inclination α is shown in Figure 24 for the quasi two-dimensional jet with $\frac{s}{d} = 1.5$. The results are compared with those of Bourque and Newman⁽²⁾, for the two-dimensional jet. It is found that the quasi two-dimensional jet reattaches further along the inclined plate than does an equivalent two-dimensional jet. Presumably, as for the circular cylinder, the attachment characteristics of the quasi two-dimensional jet depend on the hole spacing $\frac{s}{d}$. The maximum angle for reattached flow was $\alpha_{\max} \approx 55^\circ$ as compared to the two-dimensional $\alpha_{\max} = 65^\circ$ for an $\frac{l}{b_e} = 200$. As in the two-dimensional case, the flow exhibits a hysteresis phenomenon. There is a range of α for which the quasi two-dimensional jet is either reattached or fully separated depending on how it is

started. If originally reattached, it can be easily separated by obstructing it instantaneously. On the other hand, a separated jet can easily be reattached within this range of α by deflecting it toward the inclined flat plate. For the present case, the maximum value of α for which the flow spontaneously reattaches is 50° which is in very good agreement with the value for a two-dimensional jet at the same $\frac{l}{b_e}$.

6. CONCLUSIONS

The quasi two-dimensional jet becomes effectively two-dimensional approximately twelve hole spacings downstream of the holes. The actual distance $\frac{x_{2D}}{d}$ and the position of the hypothetical origin $\frac{x_0}{d}$ are both functions of the hole spacing $\frac{s}{d}$ as shown in Figure 19. For the range of hole spacings investigated, the location $\frac{x_0}{d}$ of the hypothetical origin was positive and varied with $\frac{s}{d}$. The theoretical prediction of these values, based on Reichardt's theory, is fairly satisfactory, particularly for $\frac{x_{2D}}{d}$. It is of interest to note that the hypothetical origin for a single axisymmetric jet was found to be located in the discharge plane of the hole.

It is useful to note that at any particular position the downstream velocity is higher for the quasi two-dimensional jet than for the equivalent two-dimensional jet. The velocity increases with the hole spacing $\frac{s}{d}$ and this is due to the associated downstream movement of the hypothetical origin.

The static pressures on the face of the exit plane of the holes are less than 1/2% of $(p_0 - p_\infty)$ for both the quasi two-dimensional and the two-dimensional jets. Thus the downstream momentum, which is conserved, very nearly equals the momentum at the exit plane when allowance is made for internal boundary layer growth.

At high Reynolds Numbers, the quasi two-dimensional jet separates from an adjacent circular cylinder of large radius $\frac{a}{d}$ at about 200° as compared with 240° for a thin two-dimensional jet. It also reattaches to an adjacent inclined flat plate farther downstream than does its two-dimensional counterpart for the same plate inclination. The maximum angle of inclination is less, being 55° instead of 65° at $\frac{l}{b_e} = 200$, although the maximum angle for spontaneous reattachment of an already-separated jet is similar.

The investigation of the quasi two-dimensional jet could be usefully extended in the following areas:

- (i) A more exhaustive experimental study of the details of the flow, in particular near the holes.
- (ii) An extensive theoretical and experimental investigation of the Coanda deflection of the quasi two-dimensional jet by adjacent and offset boundaries.
- (iii) A study of the quasi two-dimensional jet in streaming flow as a contribution to the design of jet-flapped wings and to the general field of boundary layer control by blowing.
- (iv) An extension to compressible flow.

APPENDIX

APPARATUS AND EXPERIMENTAL PROCEDURE

The apparatus used is shown both schematically and photographically in Figures 25, 26 27 and 28. By means of it, incompressible, turbulent jet flow from a series of closely spaced holes in line was achieved.

The air was supplied by a centrifugal compressor powered by a 10 H.P., constant speed, 3-phase induction motor. The air was filtered at the intake and the outlet of 6 in. I.D. was connected to the 6 in. diameter pipes which extend about 40 ft. from the compressor room to the Aerodynamics Laboratory above. Immediately on entering the Laboratory, the air flow was controlled by a butterfly valve with a perforated peripheral housing for bleeding off excess air. This arrangement permitted infinitely variable jet speed control from 10 to 375 ft/sec. For the lowest speeds, the butterfly valve was nearly closed, the majority of the flow then emanating through the bleed holes. On the other hand, for the higher speeds, the butterfly valve was fully opened and the bleed holes were blocked off by a sliding sleeve located around the outer periphery of the valve. Any intermediate speeds could be obtained by partial bleeding and partial opening of the valve.

From the valve the flow proceeded through a 6 in. dia. corrugated flexible duct to a 40° expansion, which flared out from a 6 in. O.D. circular section to a 6 in. × 24 in. rectangular section. The expansion itself was constructed in two parts, one being of 1/16 in. sheet steel in which the circular section gradually blended into a rectangular one of 6 in. × 18 in. cross section. A curved perforated plate was here placed approximately normal to the flow to reduce the adverse pressure gradient created by the expanding flow and prevent separation of the flow from the walls of the expansion. The second part of the expansion, downstream of the perforated plate, had plywood and plexiglass walls. A 1/2 in. thick sheet of plexiglass formed the upper wall to permit flow visualization within the expansion as indicated by wool tufts attached to the walls. The expansion terminated in a rectangular 6 in. × 24 in. section containing a 4:1 deep cell honeycomb and a final contraction.

The contraction was carried out in two stages. Two contoured hardwood fairings ensured smooth two-dimensional converging flow in the initial contraction from a section of 6 in. × 24 in. to one of 2 in. × 24 in. Thereafter, the final stage of contraction was included in the interchangeable face-blocks for each slot or hole arrangement (Figure 26). To prevent influx, adequate end-plates were provided as shown in Figure 27.

The study of the flow in the quasi two-dimensional jet involved an investigation at three hole spacings with $\frac{s}{d} = 1.5, 2.0, \text{ and } 3.0$ for a hole diameter $d = 1/2$ in. in all cases. Two $1\ 1/2$ in. thick plexiglass face-blocks, $6\ 1/2$ in. \times 24 in., were machined to give hole spacings of $\frac{s}{d} = 1.5$ and 2.0 and every alternate hole in the $\frac{s}{d} = 1.5$ face block was sealed off to give the $\frac{s}{d} = 3.0$ hole spacing. The process of machining involved pre-drilling the plexiglass plates undersize to the desired hole spacing for subsequent finishing with a $1/2$ in. dia. reamer. A specially contoured tool, shown photographically in Figure 29,* was used to machine the contraction contours to ensure a uniform distribution of the flow among the individual jets. The final $1/2$ in. length of each hole was straight, without contraction, to ensure that the flow emerged as a series of straight and uniform axisymmetric jets.

For the study of the two-dimensional jet, new contoured face-blocks were provided, as shown schematically in Figure 26. These blocks consisted of two $1/2$ in. thick plates of steel 3 in. \times 24 in. and $3\ 1/2$ in. \times 24 in. and attached to each was a contoured hardwood fairing which matched the permanently installed fairings of the initial contraction. The steel surfaces from which the flow emanated were surface ground to a tolerance of ± 0.001 in. and a

* Note Figure 29 is on the same page as Figures 16 & 17.

sharp lip was maintained to ensure that the flow emerged as a straight, uniform two-dimensional jet (no Coanda deflection). The smaller face-block (1/2 in. \times 3 in. \times 24 in.) was aligned to the lower fairing of the initial contraction to serve as the lower lip of the two-dimensional jet. The slot width was set by resting the ground surface of the larger face-block on the proper-sized gauge blocks which in turn rested on the ground surface of the lower face-block. The upper face-block was then fixed into place and the gauge blocks removed to leave a slot width with a tolerance of approximately ± 0.001 in.

Two boundary configurations were used to study the Coanda deflection of the quasi two-dimensional jet. The circular cylinder was made of a 13 in. O.D. cardboard tube 1/4 in. thick with a sector cut out so as to allow one edge to abut against the face-block above and in line with the top tips of the series of holes. The flow emerged from the holes and proceeded on to the cylinder tangentially. The surface of the cylinder was hardened by a resin coating which was subsequently polished to provide a smooth surface extending over 300°. The point of separation of the flow from the surface of the cylinder was determined by means of goose down tufts attached to the surface. The inclined flat plate was made of 3/8 in. thick plywood 4 ft. long \times 2 ft. wide. The leading edge

was chamfered at 45° so that it could abut against the face-block at the top of the holes. The boundary edges and sharp corners were sealed off at the face-block by a coating of heavy grease. The position of reattachment of the jet was determined by using small flexible tissue paper flags fixed to the surface with hinge lines perpendicular to the direction of mean flow as described by Bourque and Newman⁽²⁾.

The velocity profiles downstream of the face-blocks were measured with a round Pitot tube with internally sharpened lips and an external diameter of 0.028 in., whose calibration curve in pitch and yaw is given in Figure 30. The velocity profiles at the slots or holes were measured with a flattened Pitot tube with internally sharpened lips and an external width of 0.007 in. A traversing gear, incorporating rails and a double-ended dial gauge, was used to permit accurate location of the measuring devices.

To determine the velocity profiles, the Pitot pressures were referenced to atmosphere and measured to an estimated accuracy of one percent by means of a large vertical alcohol manometer or an inclined alcohol manometer depending on the speed of flow. The face static pressures along the surface of the face blocks were measured with a precision alcohol manometer which could be inclined to give an

amplification of 25:1. The box pressure was measured from one of three pressure taps spaced 6 in. apart as shown in Figure 28. The three guage pressures thus obtained were equal, within the accuracy of measurement.

REFERENCES

1. Alexander, L.G.,
Baron, T.,
and Comings, E.W. Transport of Momentum, Mass, and Heat
in Turbulent Jets,
Engineering Experiment Station Bulletin
No. 413, University of Illinois, 1953.
2. Bourque, C.
and Newman, B.G. Reattachment of a Two-Dimensional
Incompressible Jet to an Adjacent Flat
Plate,
Aeronautical Quarterly, Vol. XI, p. 231,
(Aug. 1960).
3. Förthmann, E. Uber Turbulente Strahlausbreitung,
Ing.-Arch., 5, 42 (1934);
N.A.C.A. TM 789 (1936).
4. Görtler, H. Berechnung von Aufgaben der Freien
Turbulenz auf Grund Eines Neuen
Näherungsansatzes,
Z. angew. Math. Mech., 22, 244 (1942).
5. Miller, D.R.
and Comings, E.W. Static Pressure Distribution in the
Free Turbulent Jet,
Journal of Fluid Mechanics, Vol. 3,
(1957), p. 1-16.
6. Miller, D.R.
and Comings, E.W. Force-Momentum Fields in a Dual-Jet
Flow,
Journal of Fluid Mechanics, Vol. 7,
(1960), p. 237-256.
7. Newman, B.G. The Deflexion of Plane Jets by
Adjacent Boundaries-Coanda Effect,
Boundary-Layer Control - Principles
and Applications, edited by G.V.
Lachmann, Pergamon Press, 1961, p. 232.
8. Poisson-Quinton, Ph.
and Lepage, L. Survey of French Research on the
Control of Boundary Layer and
Circulation, Boundary-Layer Control -
Principles and Applications,
edited by G.V. Lachmann,
Pergamon Press, 1961, p. 21.
9. Reichardt, H. On a New Theory of Free Turbulence,
J. Roy. Aero. Soc., 47, 167.
10. Rouse, H. Advanced Mechanics of Fluids, p. 359,
John Wiley and Sons, (1959).

11. Sawyer, R.A. The Flow Due to a Two-Dimensional Jet Issuing Parallel to a Flat Plate, Journal of Fluid Mechanics, Vol. 9, (1960).
12. Schlichting, H. Boundary-Layer Theory, p. 590, McGraw-Hill Book Co., (1960).
13. Tollmien, W. Berechnung Turbulenter Ausbreitungsvorgänge, Z. angew. Math. Mech., 6, 468 (1926); N.A.C.A. TM 1085 (1945).
14. Townsend, A.A. The Structure of Turbulent Shear Flow, Cambridge University Press (1956).

VARIATION OF C_m WITH DOWNSTREAM DISTANCE
FOR AN AXISYMMETRIC JET

$$d = 0.500 \text{ in.}, R_e = \left[\frac{(p_0 - p_\infty) d^2}{\rho v^2} \right]^{\frac{1}{2}} = 2.1 \times 10^6$$

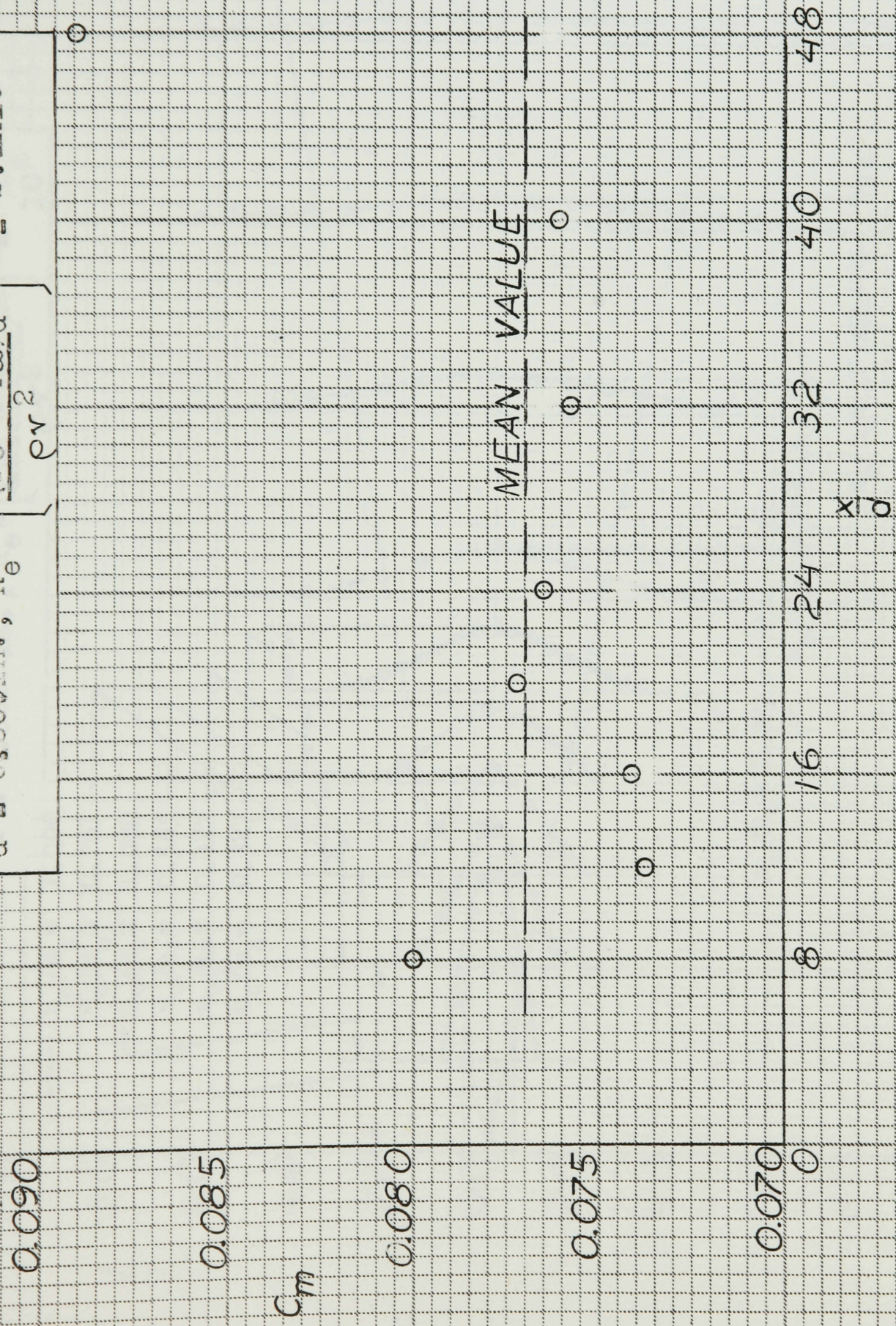
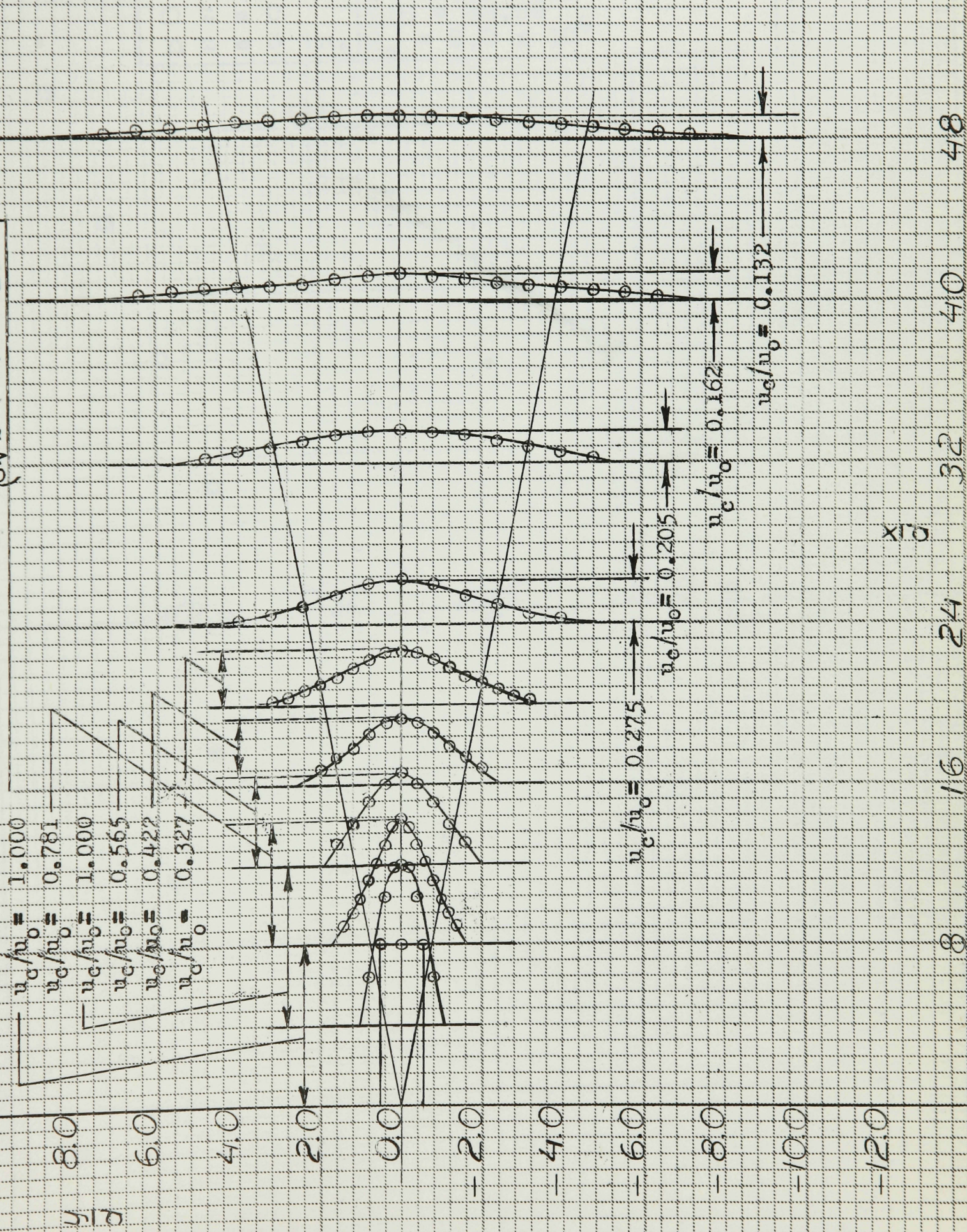


FIG. 2

FIG. 3

EXPERIMENTAL MEAN VELOCITY PROFILES IN THE
CENTERPLANE $z = 0$ OF THE AXISYMMETRIC
JET

$d = 0.500$ in., $Re = \left[\frac{(\rho_0 - \rho_\infty) d^2}{\rho r^2} \right]^{\frac{1}{2}} \times 10^6$



8 16 24 32 40 48

FIG. 4

EXPERIMENTAL MEAN VELOCITY PROFILES
 FOR A TWO-DIMENSIONAL JET IN
 PLANES $z = 0$ and $z = 3$ in.
 $\circ z = 0$ } $b = 0.245$ in.
 $\triangle z = 3$ in. } $x/b = 48.98$
 $R_e = 2.0 \times 10^6$

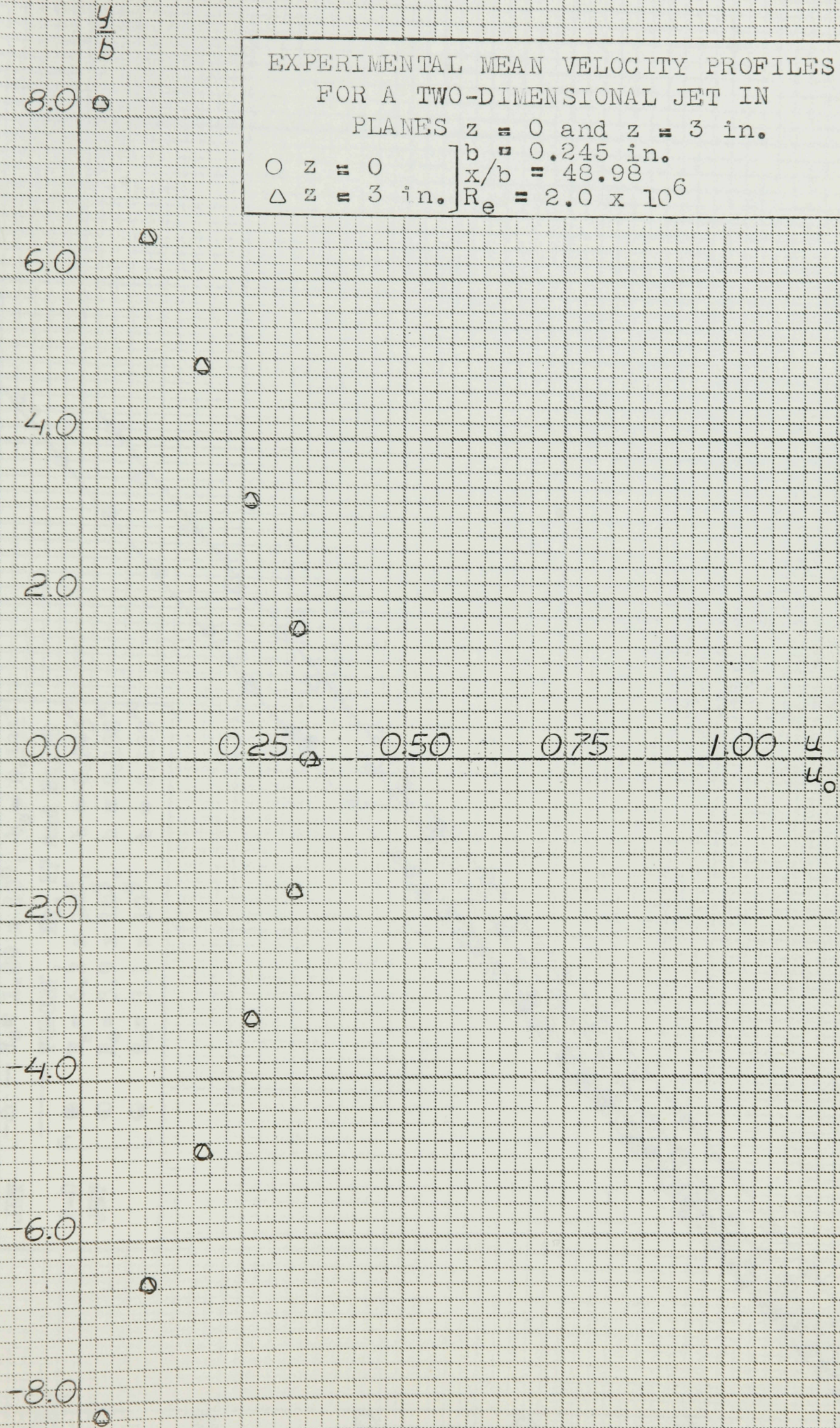


FIG. 5

INVERSE SQUARES OF MAXIMUM MEAN
VELOCITY PLOTTED AGAINST DOWNSTREAM
DISTANCE

DISTANCE

QUASI	—○—	$Re = 1.68 \times 10^6$	$b_e = 0.262$
2-D	—◇—	$Re = 1.66 \times 10^6$	$b_e = 0.196$
JET	—△—	$Re = 1.89 \times 10^6$	$b_e = 0.131$
— THEORY, Eq. 27 and Eq. 28 —			
2-D	●	$Re = 6.2 \times 10^5$	$b = 0.245$
JET	⊙	$Re = 3.9 \times 10^5$	$b = 0.188$
	⊖	$Re = 3.1 \times 10^5$	$b = 0.123$

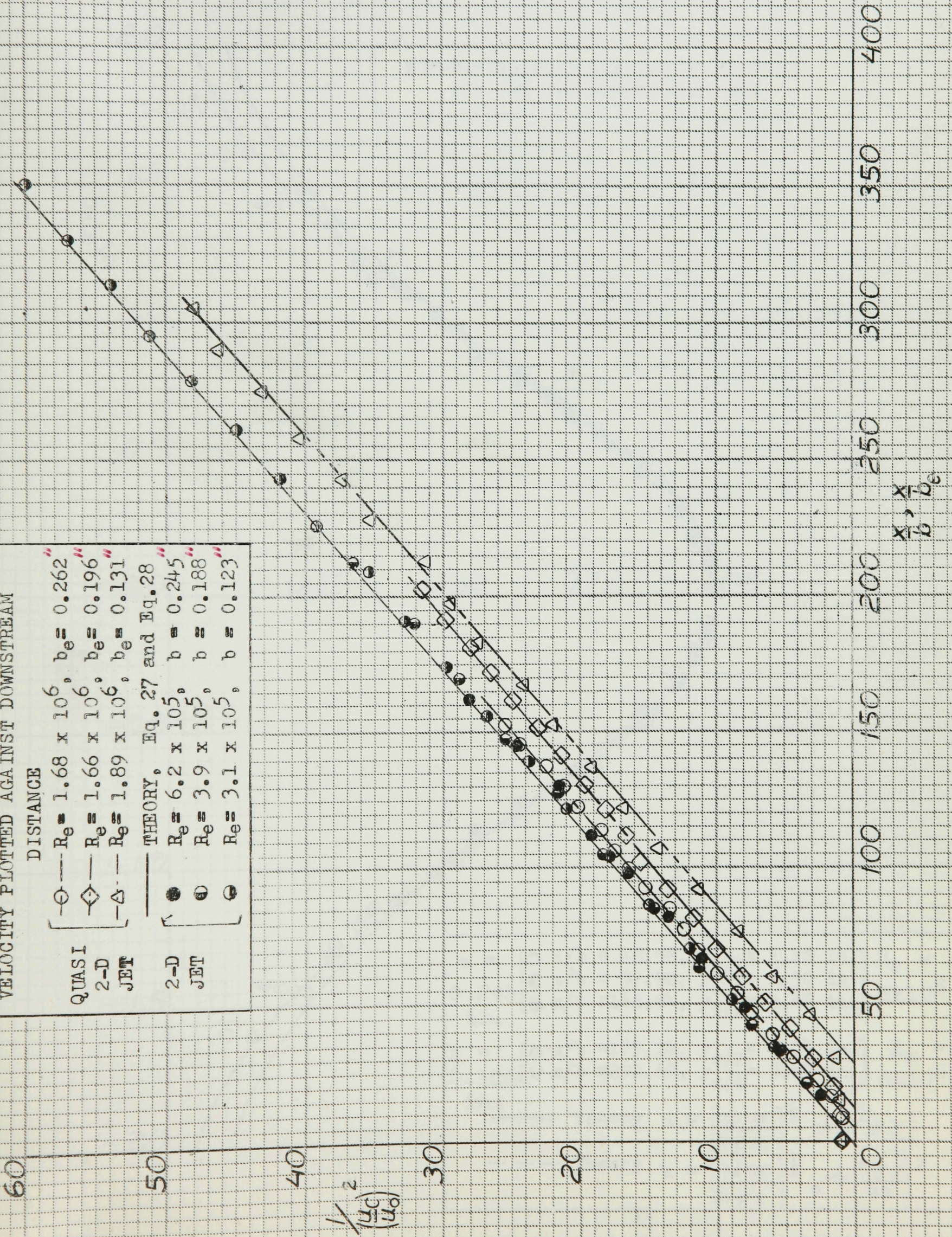
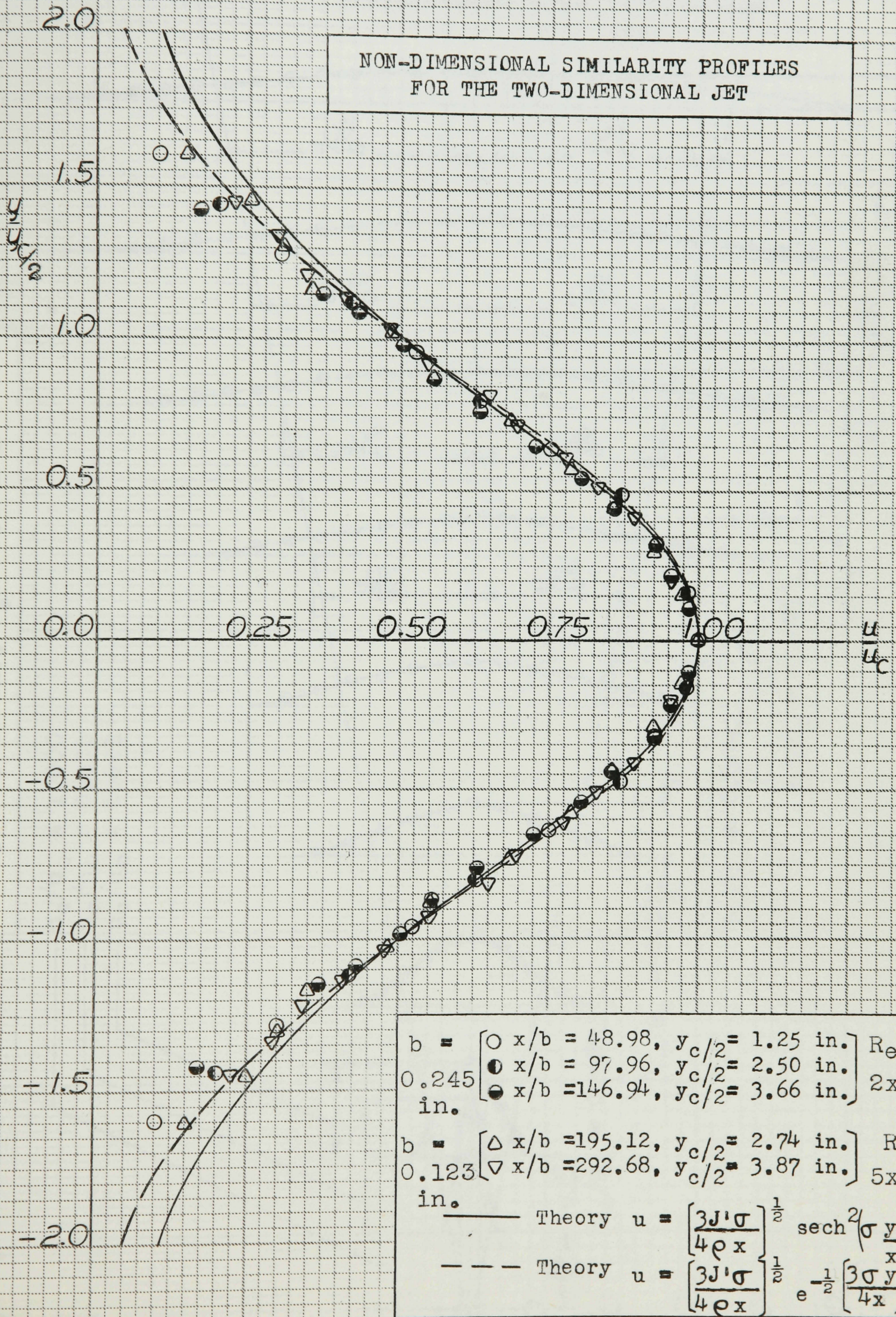


FIG. 6



EXPERIMENTAL MEAN VELOCITY PROFILES
 IN THE CENTERPLANE $z = 0$ OF THE
 2-D JET

$b = 0.245$ in., $Re = 2.0 \times 10^6$

$u_c/u_0 = 1.000$
 $u_c/u_0 = 0.875$
 $u_c/u_0 = 0.641$

y/b
 24.0
 20.0
 16.0
 12.0
 8.0
 4.0
 0.0
 -4.0
 -8.0
 -12.0
 -16.0
 -20.0
 -24.0

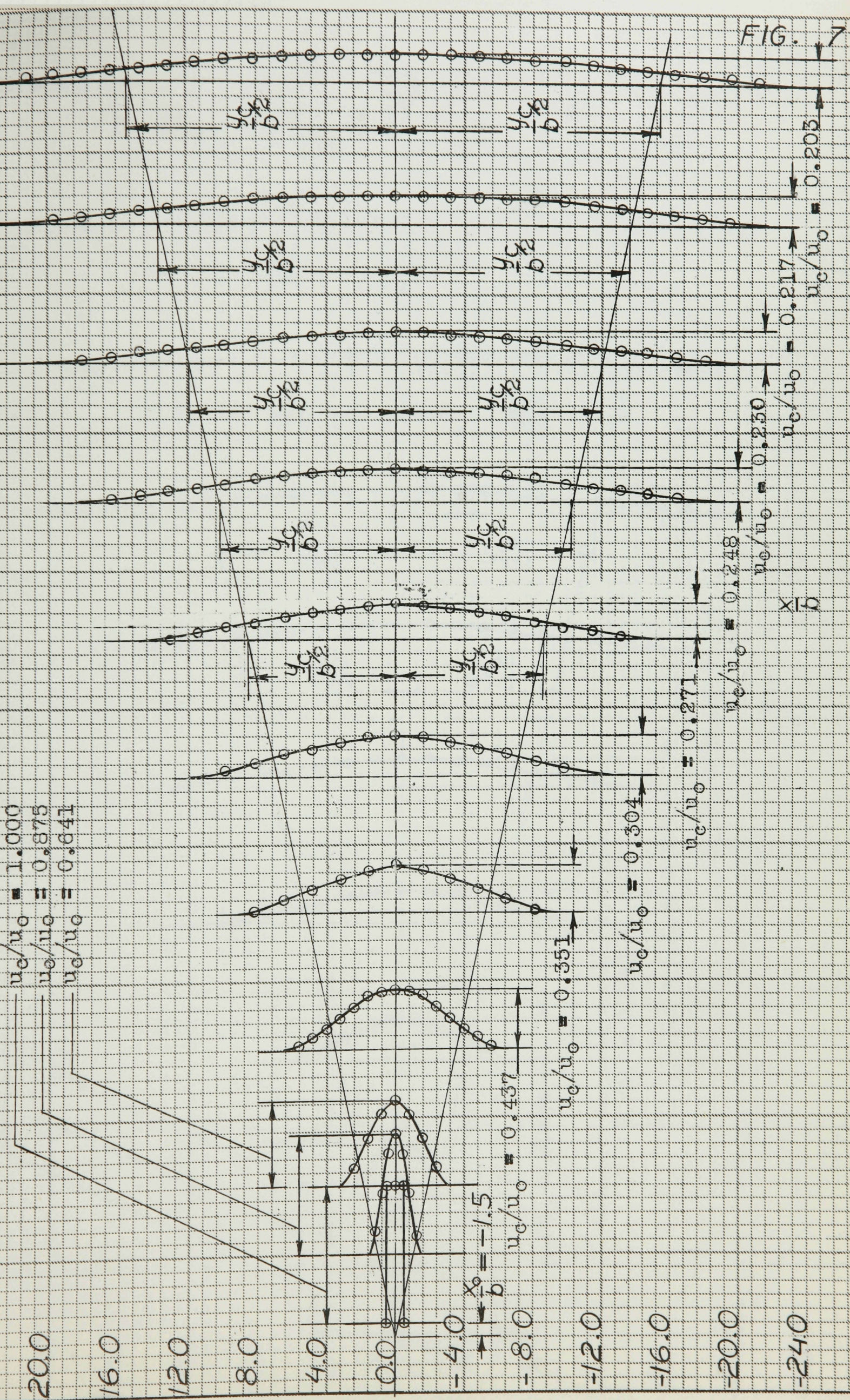


FIG. 7

EXPERIMENTAL MEAN VELOCITY PROFILES
 IN THE CENTERPLANE $z = 0$ OF THE
 2-D JET

$b = 0.123$ in., $Re = 5.0 \times 10^5$

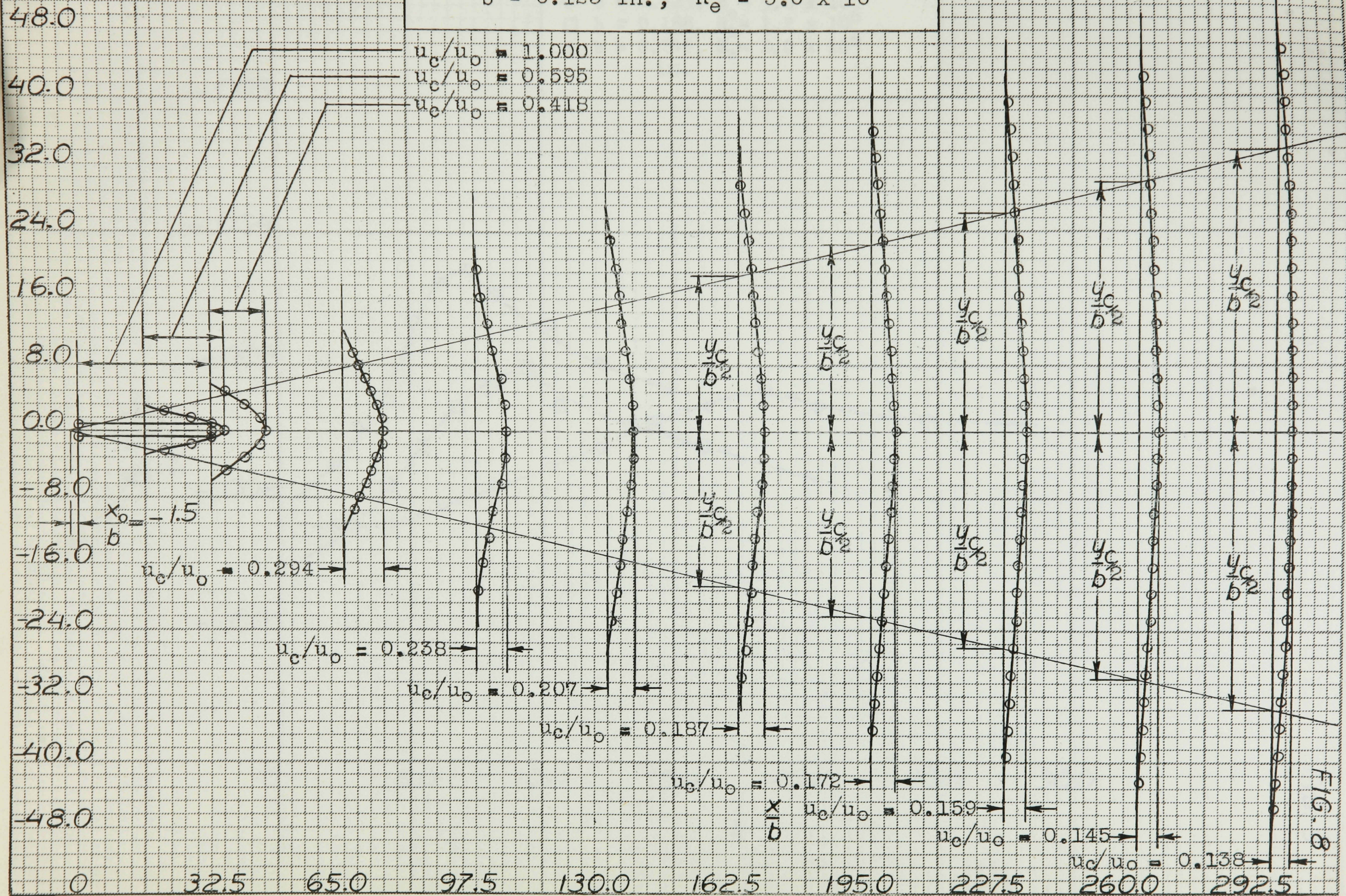
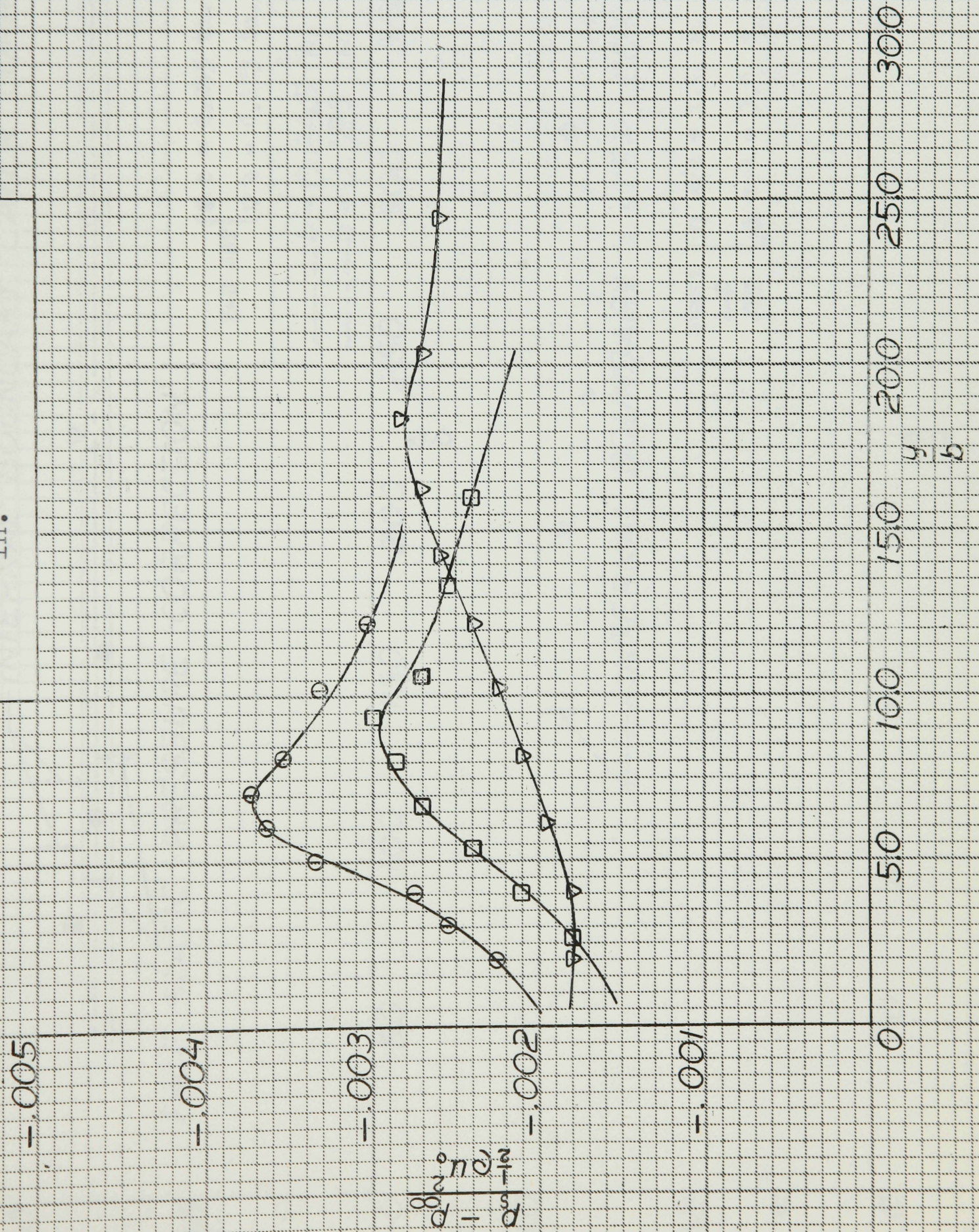


FIG. 8

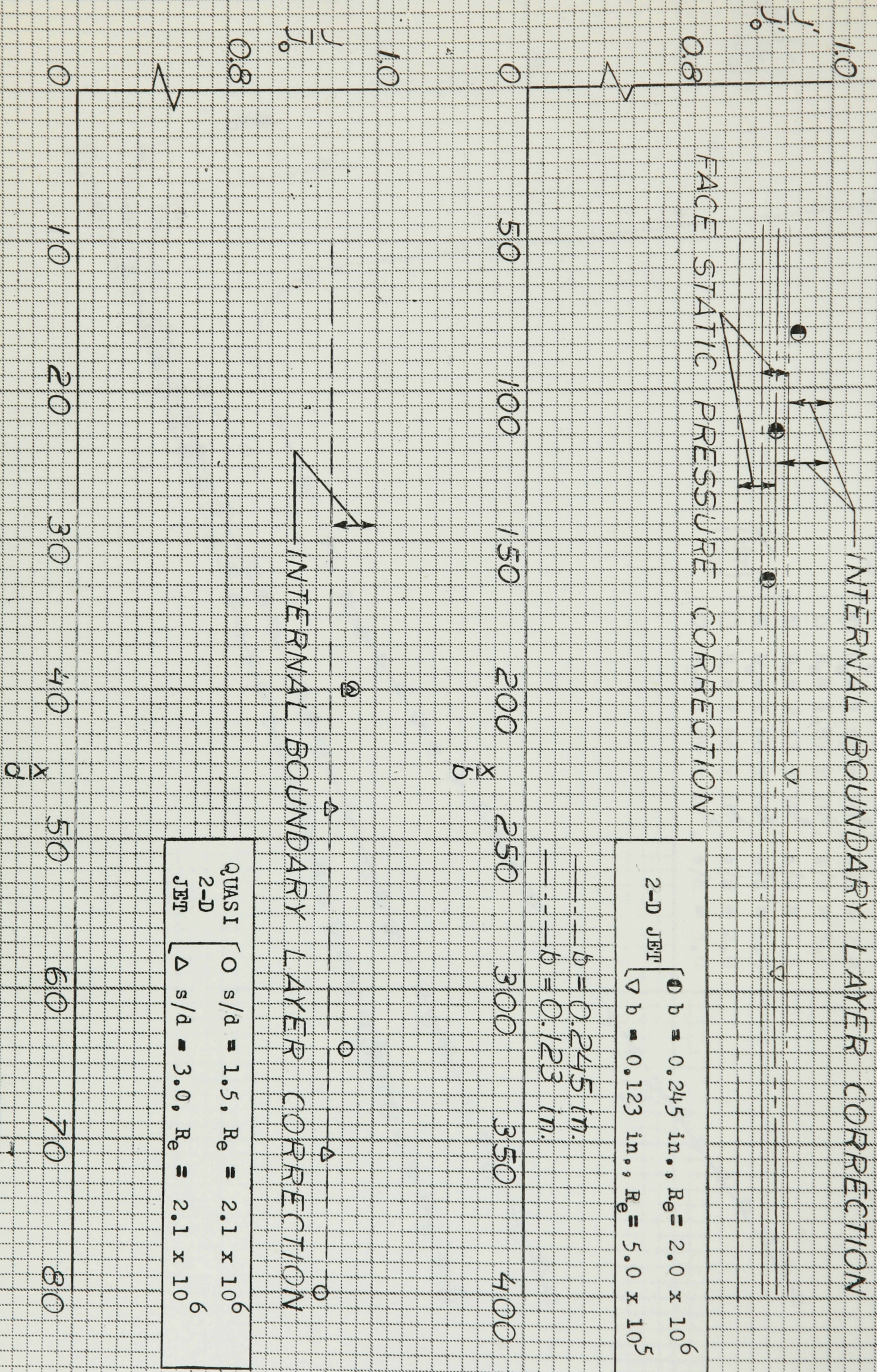
FIG. 9

STATIC PRESSURE ON THE SURFACE
OF THE FACE-BLOCK OF THE
2-D JET

- ∇ $b = 0.123, Re = 5.0 \times 10^5$
 - \square $b = 0.188, Re = 1.2 \times 10^6$
 - \oplus $b = 0.245, Re = 2.0 \times 10^6$
- in.



CONSERVATION OF DOWNSTREAM MOMENTUM IN THE
QUASI 2-D AND IN THE 2-D JETTS



2-D JET
 \circ $b = 0.245 \text{ in.}, Re = 2.0 \times 10^6$
 ∇ $b = 0.123 \text{ in.}, Re = 5.0 \times 10^5$

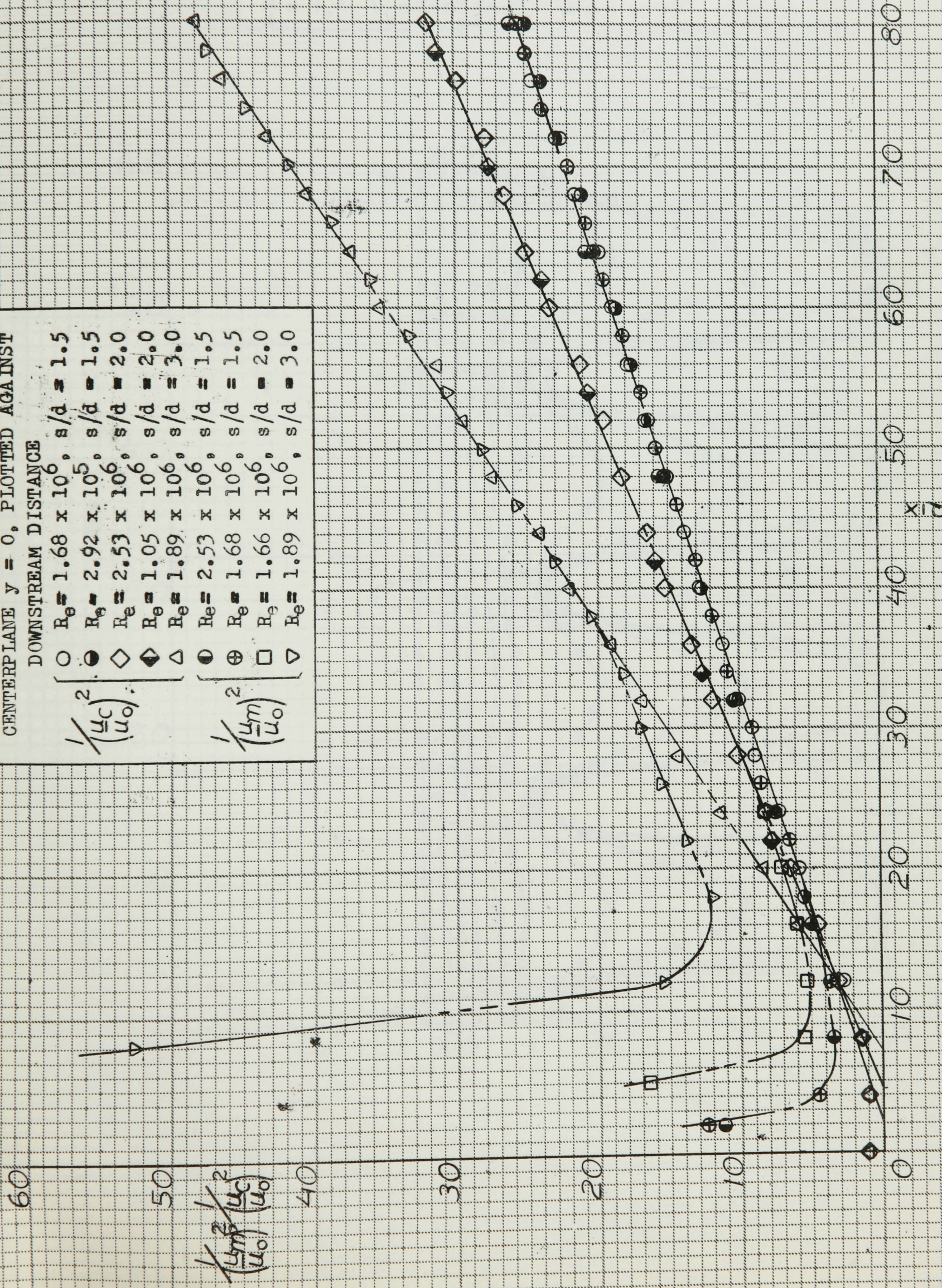
— $b = 0.245 \text{ m.}$
 - - - $b = 0.123 \text{ m.}$

QUASI 2-D
 JET
 \circ $s/d = 1.5, Re = 2.1 \times 10^6$
 ∇ $s/d = 3.0, Re = 2.1 \times 10^6$

FIG. 10

INVERSE SQUARES OF MAXIMUM AND
MINIMUM MEAN VELOCITIES IN THE
CENTERPLANE $y = 0$, PLOTTED AGAINST
DOWNSTREAM DISTANCE

\circ	$Re = 1.68 \times 10^6$	$s/d = 1.5$
\ominus	$Re = 2.92 \times 10^5$	$s/d = 1.5$
\diamond	$Re = 2.53 \times 10^6$	$s/d = 2.0$
\blacktriangle	$Re = 1.05 \times 10^6$	$s/d = 2.0$
\triangle	$Re = 1.89 \times 10^6$	$s/d = 3.0$
\bullet	$Re = 2.53 \times 10^6$	$s/d = 1.5$
\oplus	$Re = 1.68 \times 10^6$	$s/d = 1.5$
\square	$Re = 1.66 \times 10^6$	$s/d = 2.0$
∇	$Re = 1.89 \times 10^6$	$s/d = 3.0$



EXPERIMENTAL MEAN VELOCITY PROFILES
 IN THE CENTERPLANE $y = 0$

FIG. 12

$\frac{s}{d} = 1.5, Re = \frac{(\rho_0 - \rho_\infty) d^2}{\mu v} = 2.1 \times 10^6$

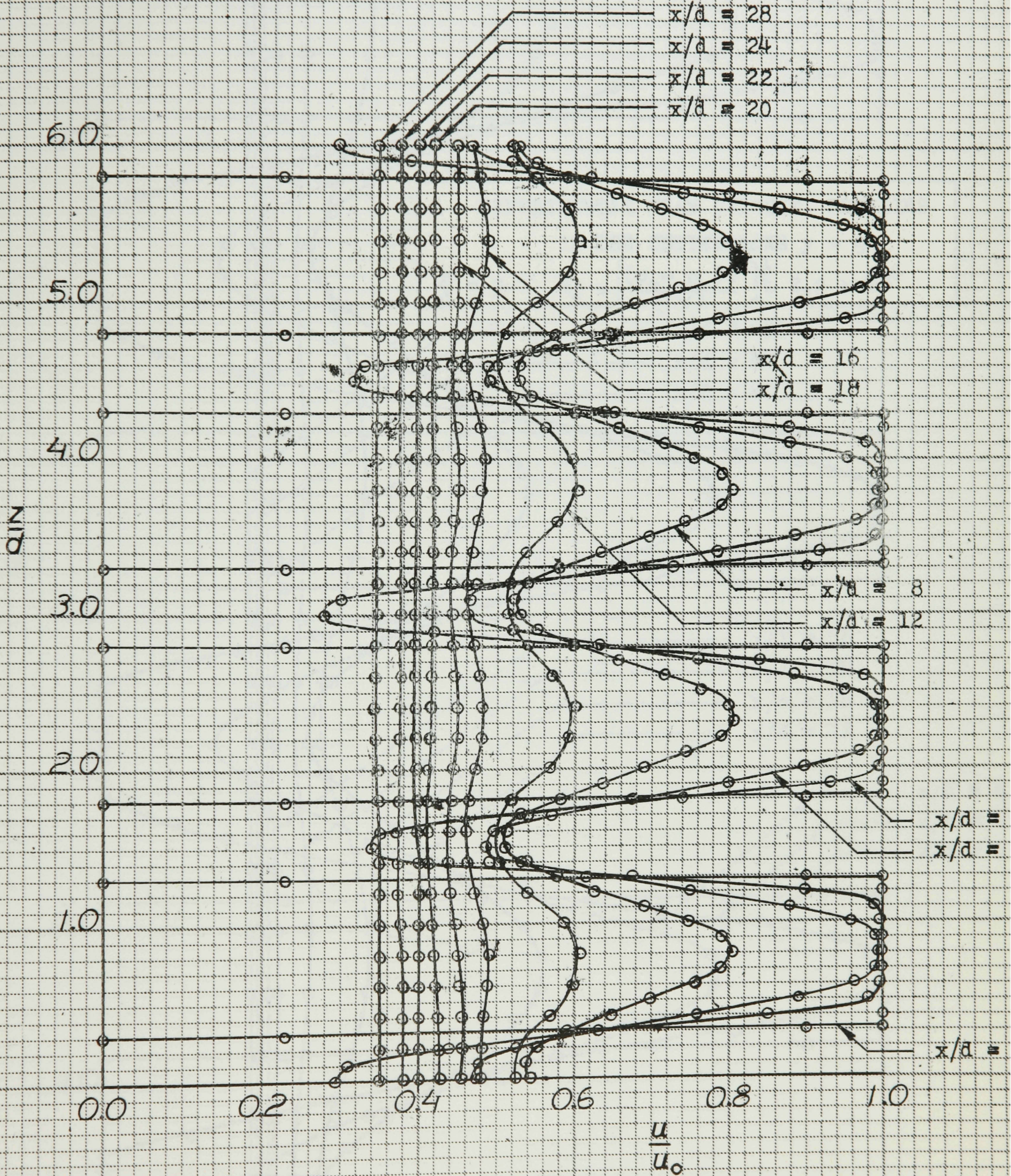


FIG. 13

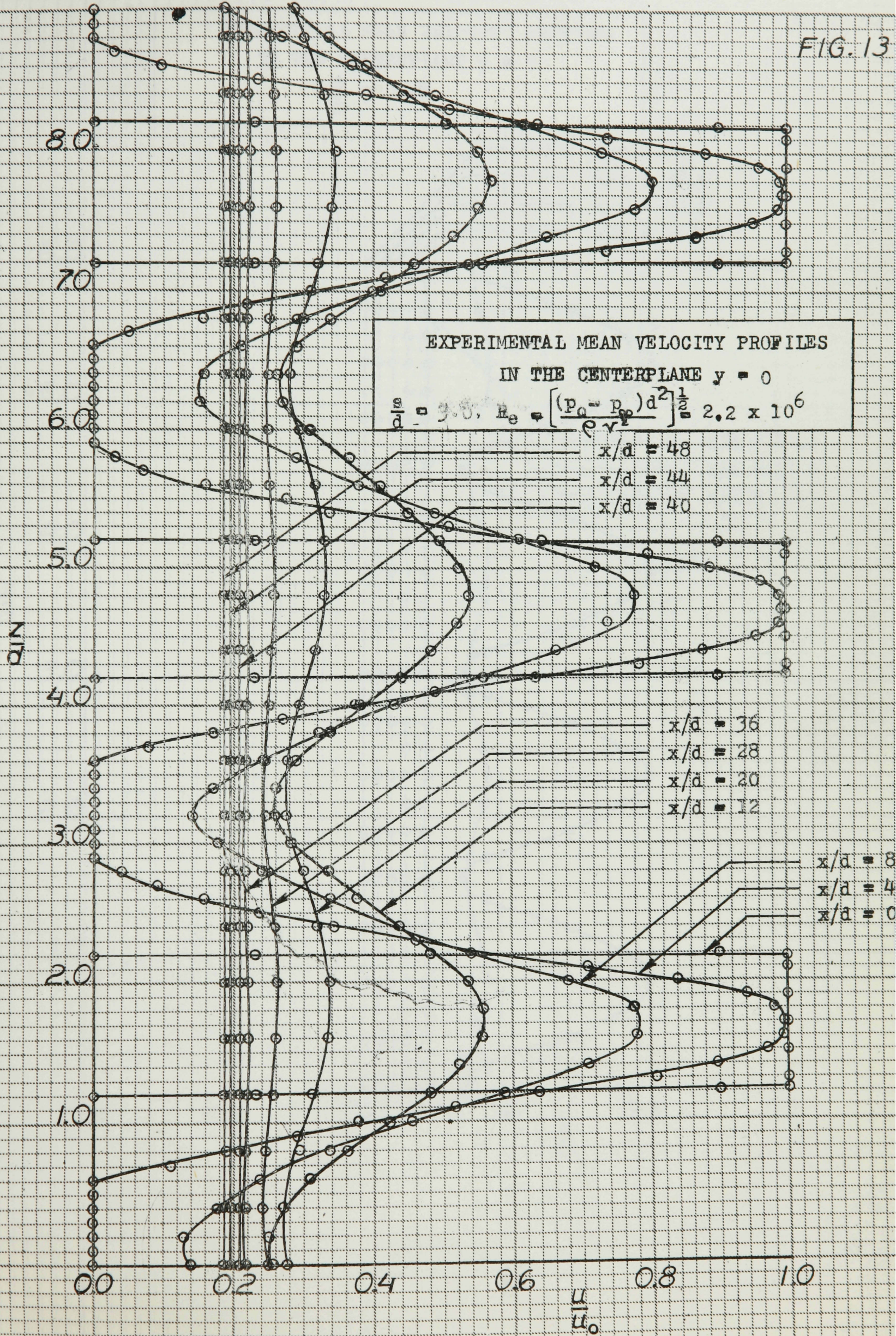
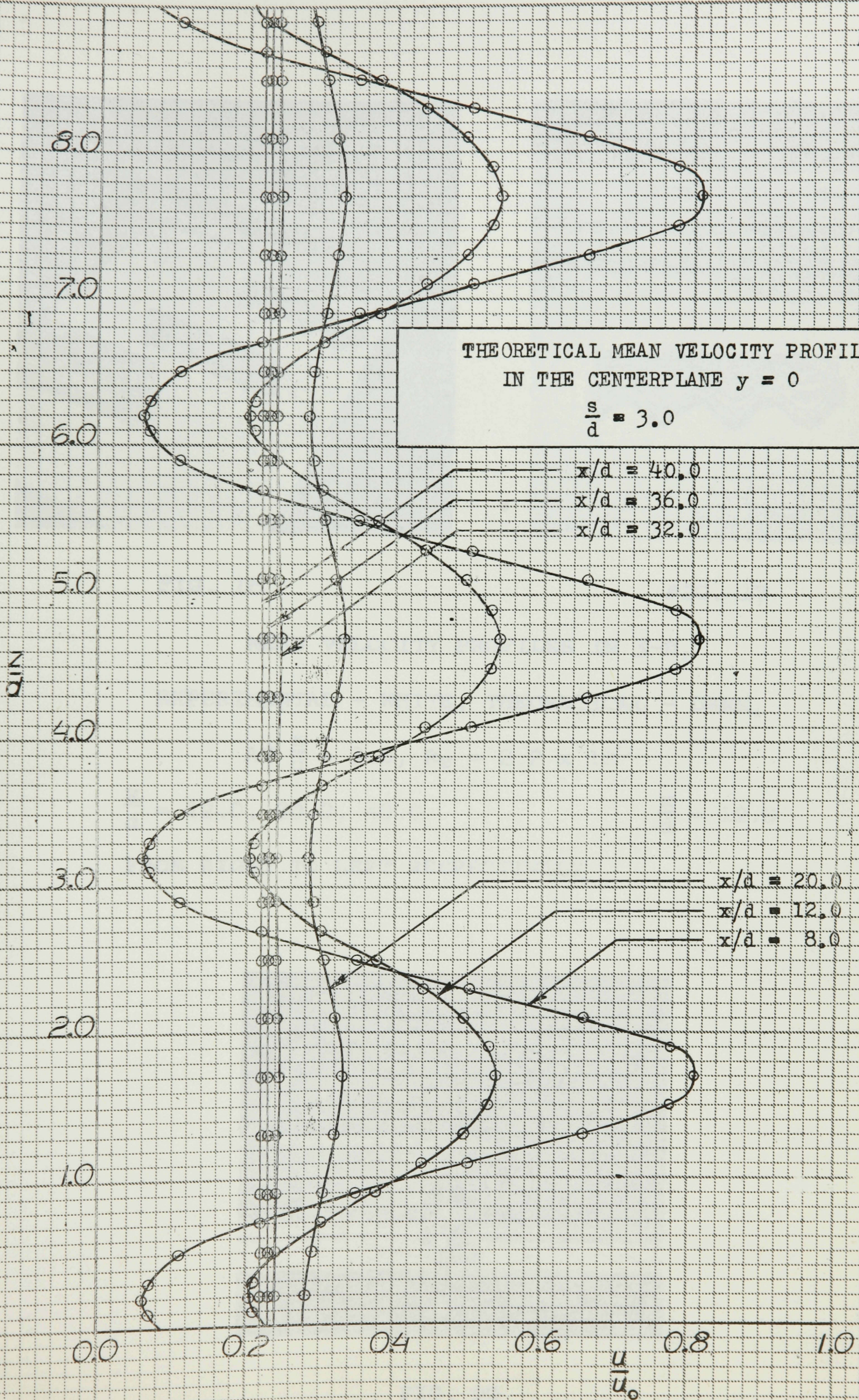


FIG. 15



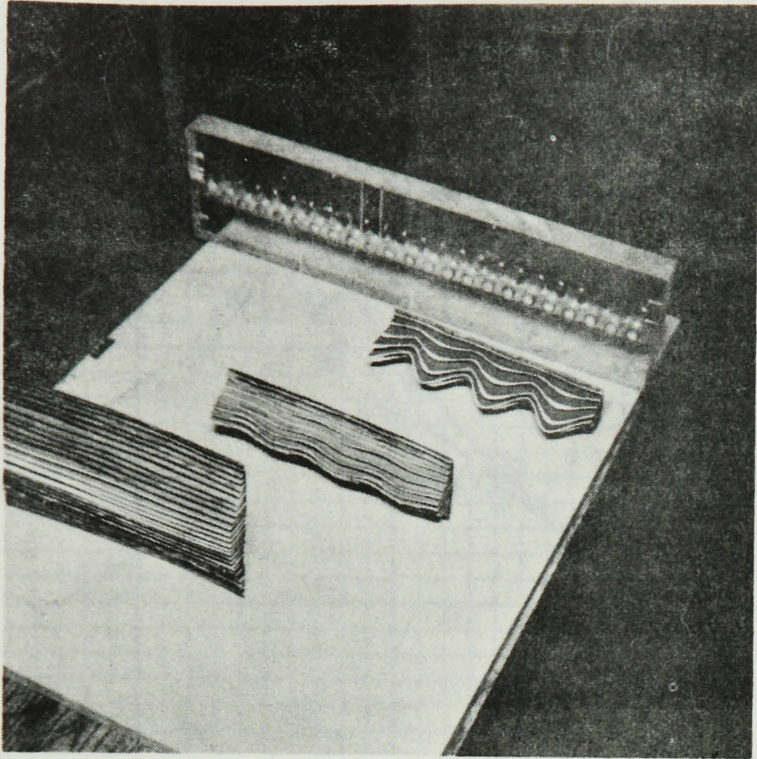


FIG. 16

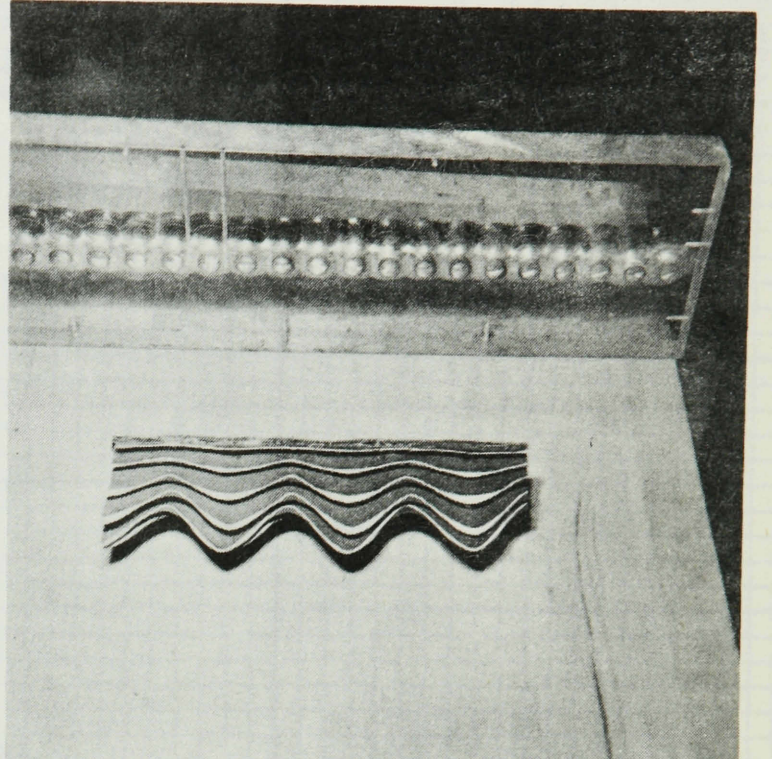


FIG. 17

MEAN VELOCITY PROFILES IN 3-D,

EXPERIMENTAL - WHITE, THEORETICAL - DARK,

AT $\frac{s}{d} = 3.0$, $Re = 2.2 \times 10^6$

$\frac{x}{d} = 12.0, 20.0, 40.0$

$\frac{x}{d} = 12.0$

FROM RIGHT TO LEFT RESPECTIVELY

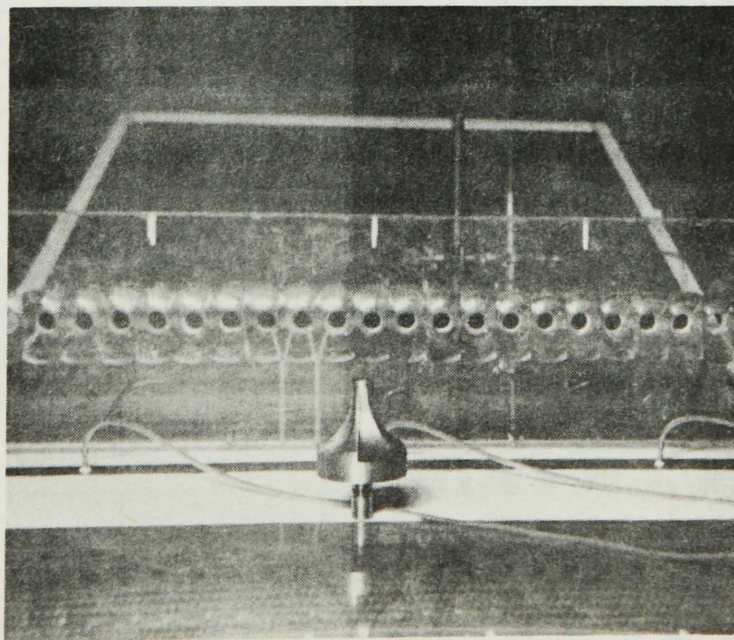
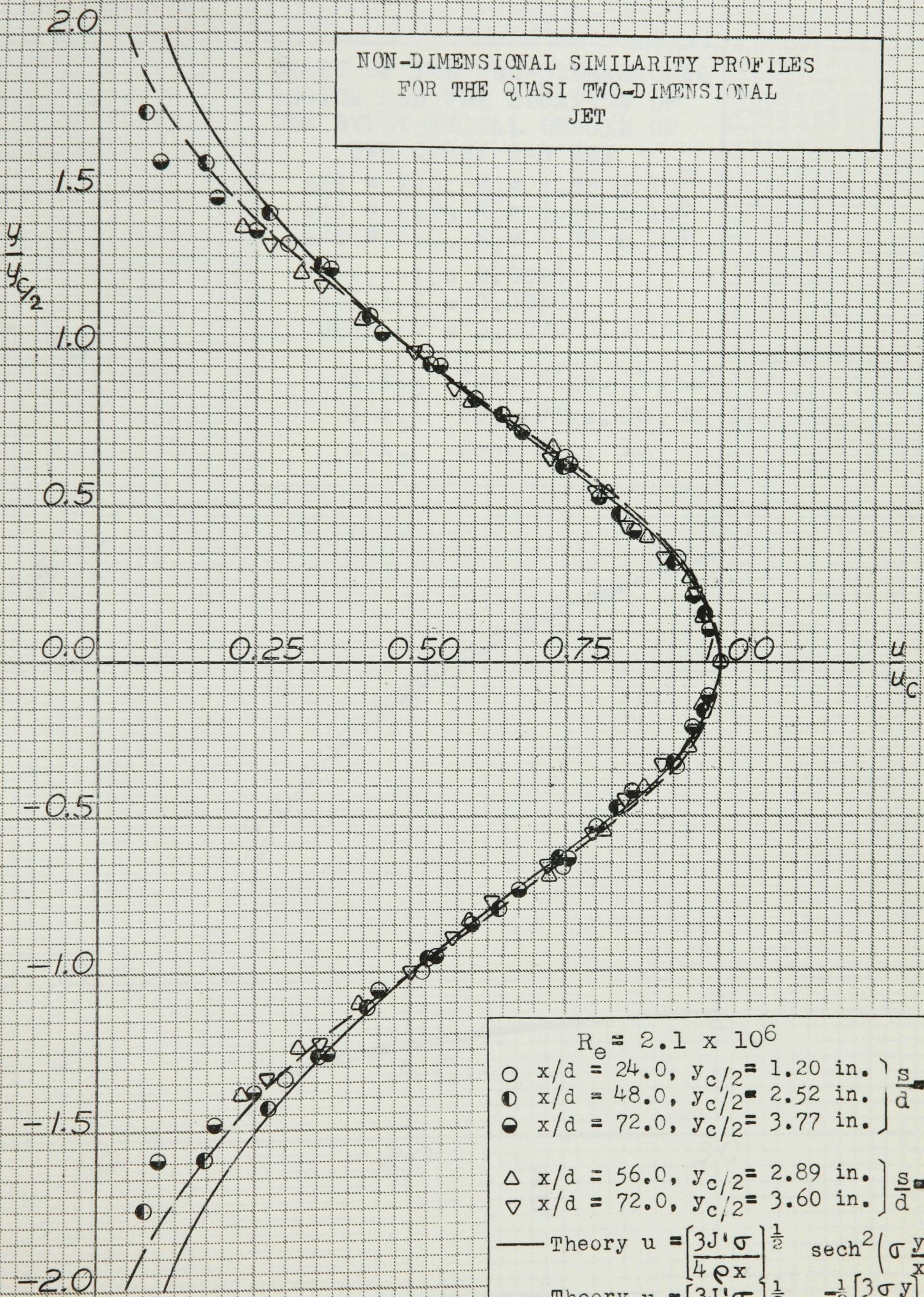


FIG. 29

CUTTER USED TO MACHINE THE CONTRACTION CONTOURS
WHICH ARE SHOWN IN THE REAR VIEW OF FACE BLOCK ($\frac{s}{d} = 1.5$)



NON-DIMENSIONAL SIMILARITY PROFILES
FOR THE QUASI TWO-DIMENSIONAL
JET

$Re = 2.1 \times 10^6$

○	$x/d = 24.0, y_c/2 = 1.20 \text{ in.}$	} $\frac{s}{d} = 1.5$
●	$x/d = 48.0, y_c/2 = 2.52 \text{ in.}$	
◐	$x/d = 72.0, y_c/2 = 3.77 \text{ in.}$	
△	$x/d = 56.0, y_c/2 = 2.89 \text{ in.}$	} $\frac{s}{d} = 3.0$
▽	$x/d = 72.0, y_c/2 = 3.60 \text{ in.}$	

— Theory $u = \left[\frac{3J'\sigma}{4\rho x} \right]^{1/2} \text{sech}^2 \left(\frac{\sigma y}{x} \right)$

-- Theory $u = \left[\frac{3J'\sigma}{4\rho x} \right]^{1/2} e^{-\frac{1}{2} \left[\frac{3\sigma y}{4x} \right]^2}$

FIG. 19

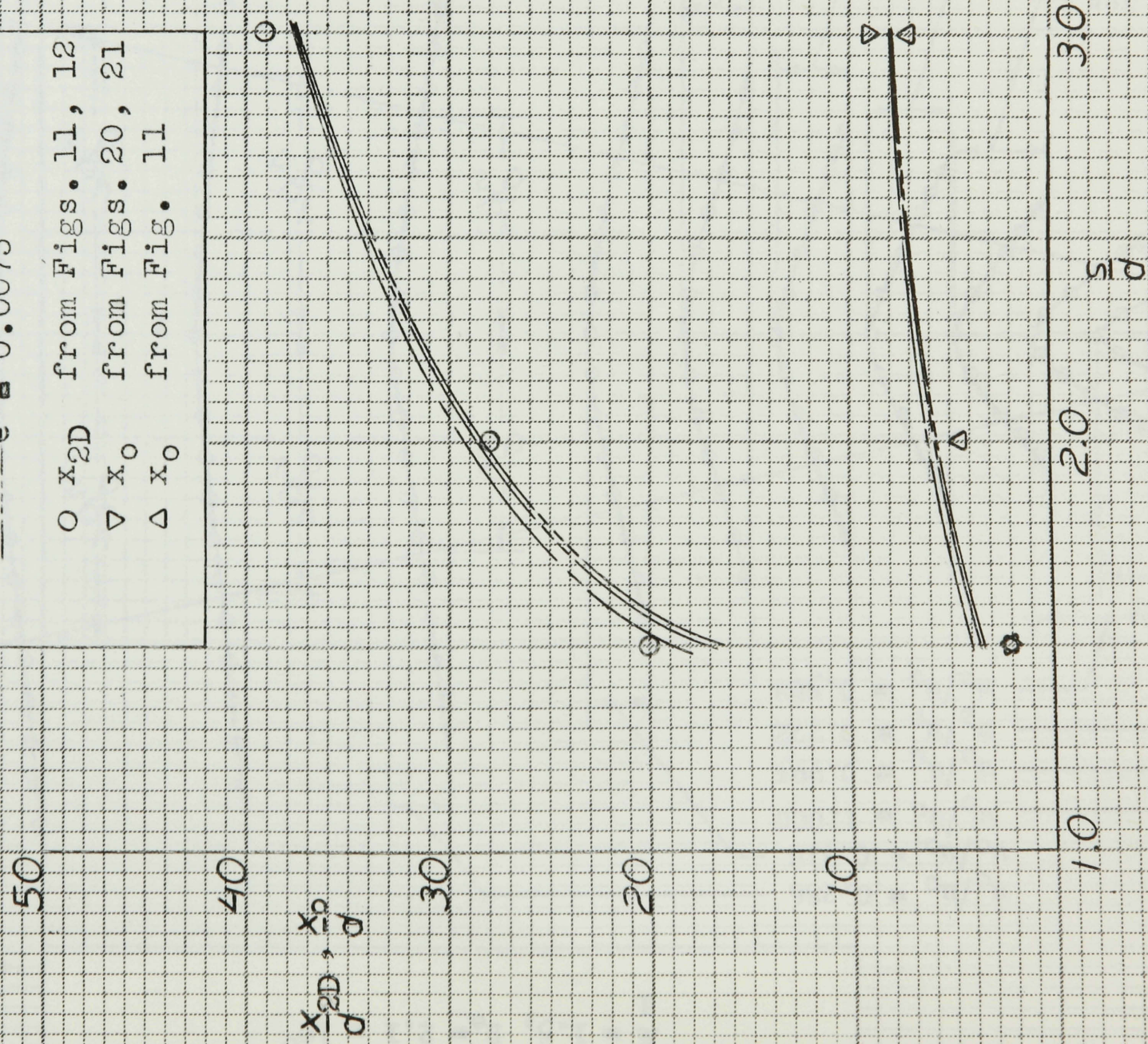
START OF THE TWO-DIMENSIONAL
 REGION AND THE LOCATION OF
 THE HYPOTHETICAL ORIGIN OF

THE QUASI 2-D JET

$s/d = 1.5, Re = 1.68 \times 10^6$
 $s/d = 2.0, Re = 2.53 \times 10^6$
 $s/d = 3.0, Re = 1.89 \times 10^6$

— $\epsilon = 0.0025$
 --- $\epsilon = 0.0050$
 - - - $\epsilon = 0.0075$

○ x_{2D} from Figs. 11, 12
 ▽ x_0 from Figs. 20, 21
 △ x_0 from Fig. 11



EXPERIMENTAL MEAN VELOCITY PROFILES IN THE
CENTERPLANE $z = 0$ OF THE QUASI 2-D JET

$\frac{s}{d} = 1.5, Re = 2.1 \times 10^6$

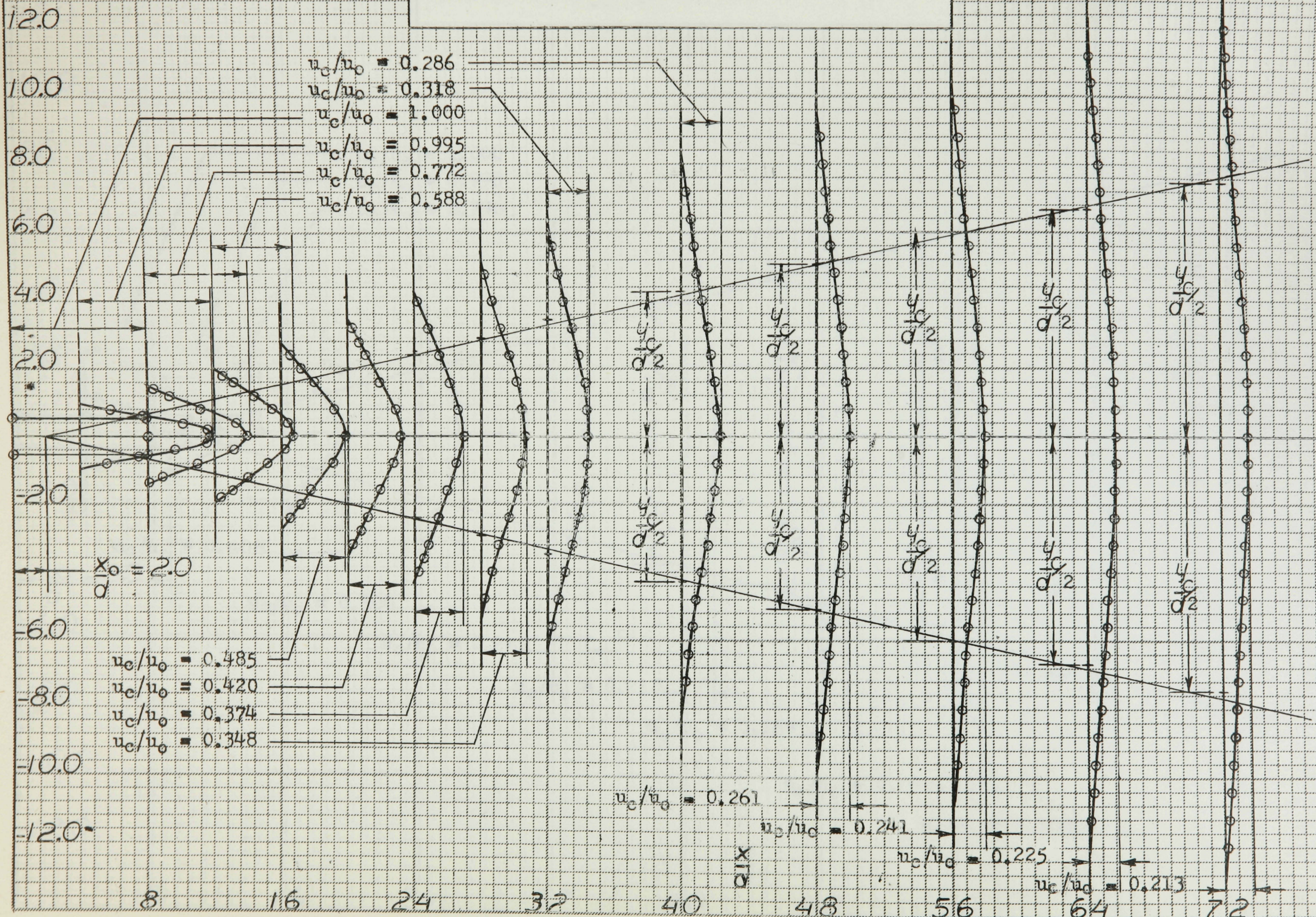


FIG. 20

FIG. 21

EXPERIMENTAL MEAN VELOCITY PROFILES IN THE
 CENTERPLANE $z = 0$ OF THE QUASI 2-D JET
 $\frac{s}{d} = 3.0, Re = 2.1 \times 10^6$

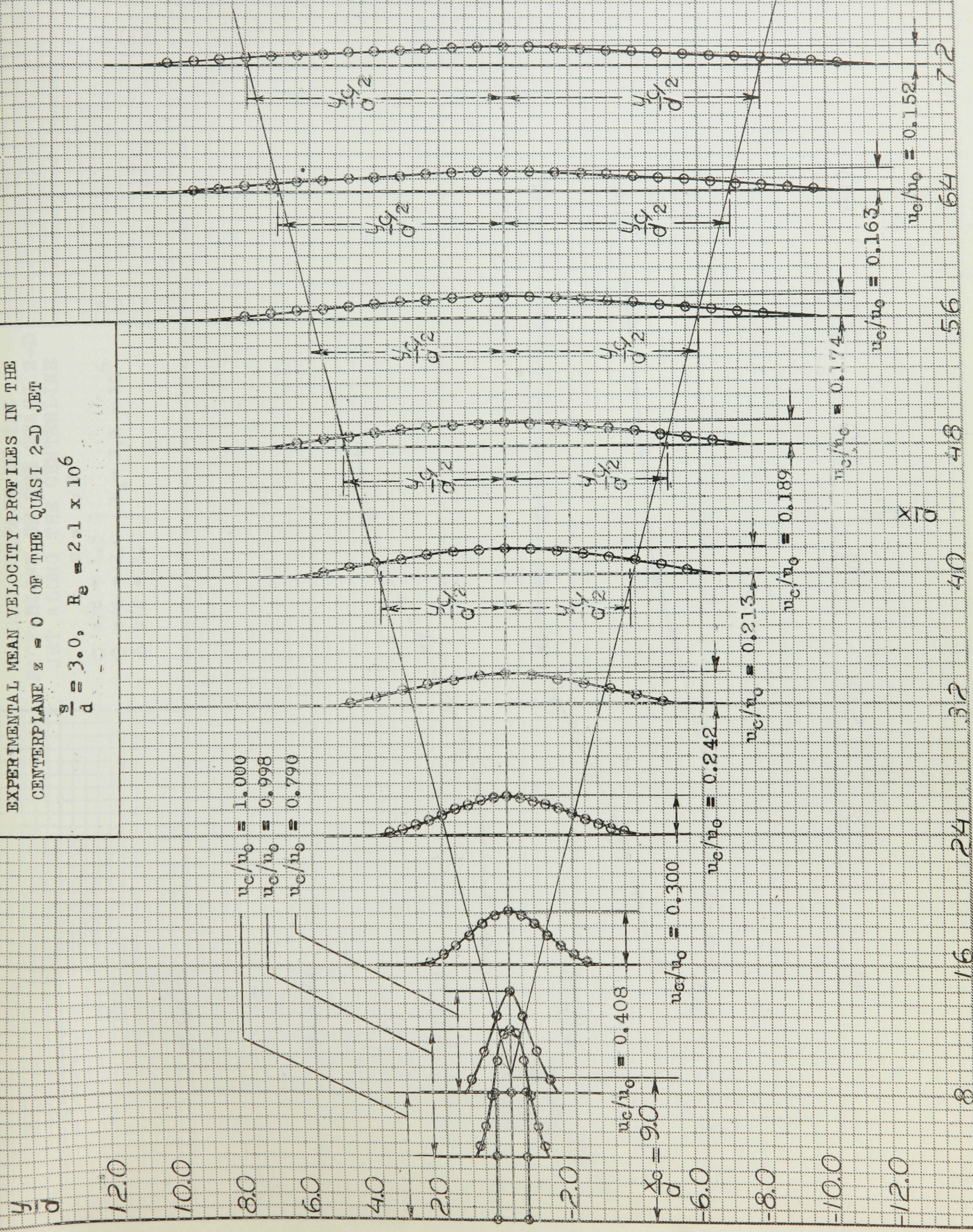


FIG. 22

STATIC PRESSURE MEASURED ON
 THE SURFACE OF THE
 FACE-BLOCK OF THE QUASI 2-D
 JET ALONG THE CENTERLINE
 $z = s/2$
 $\circ \quad s/d = 1.5$
 $\diamond \quad s/d = 2.0$
 $\triangle \quad s/d = 3.0$

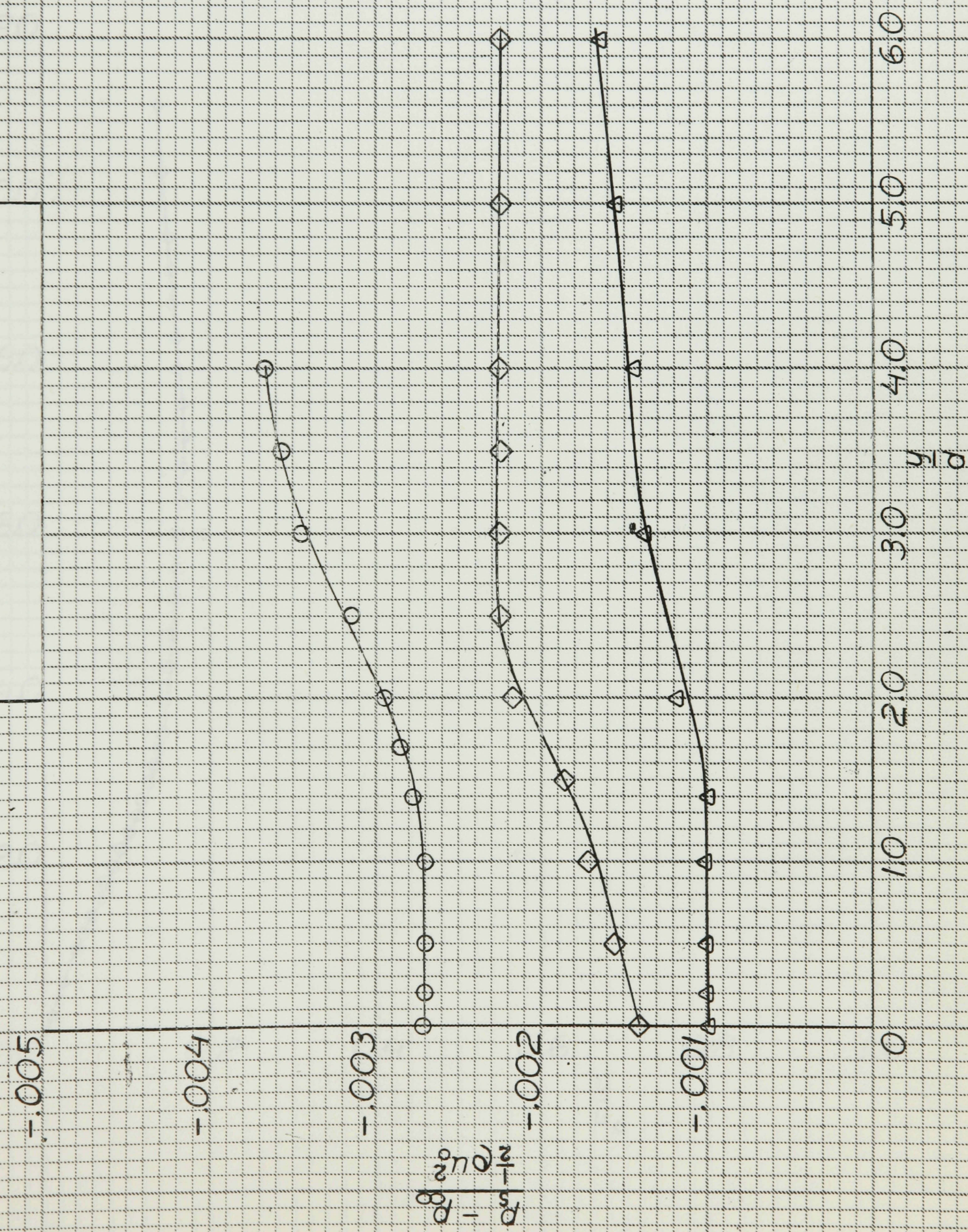
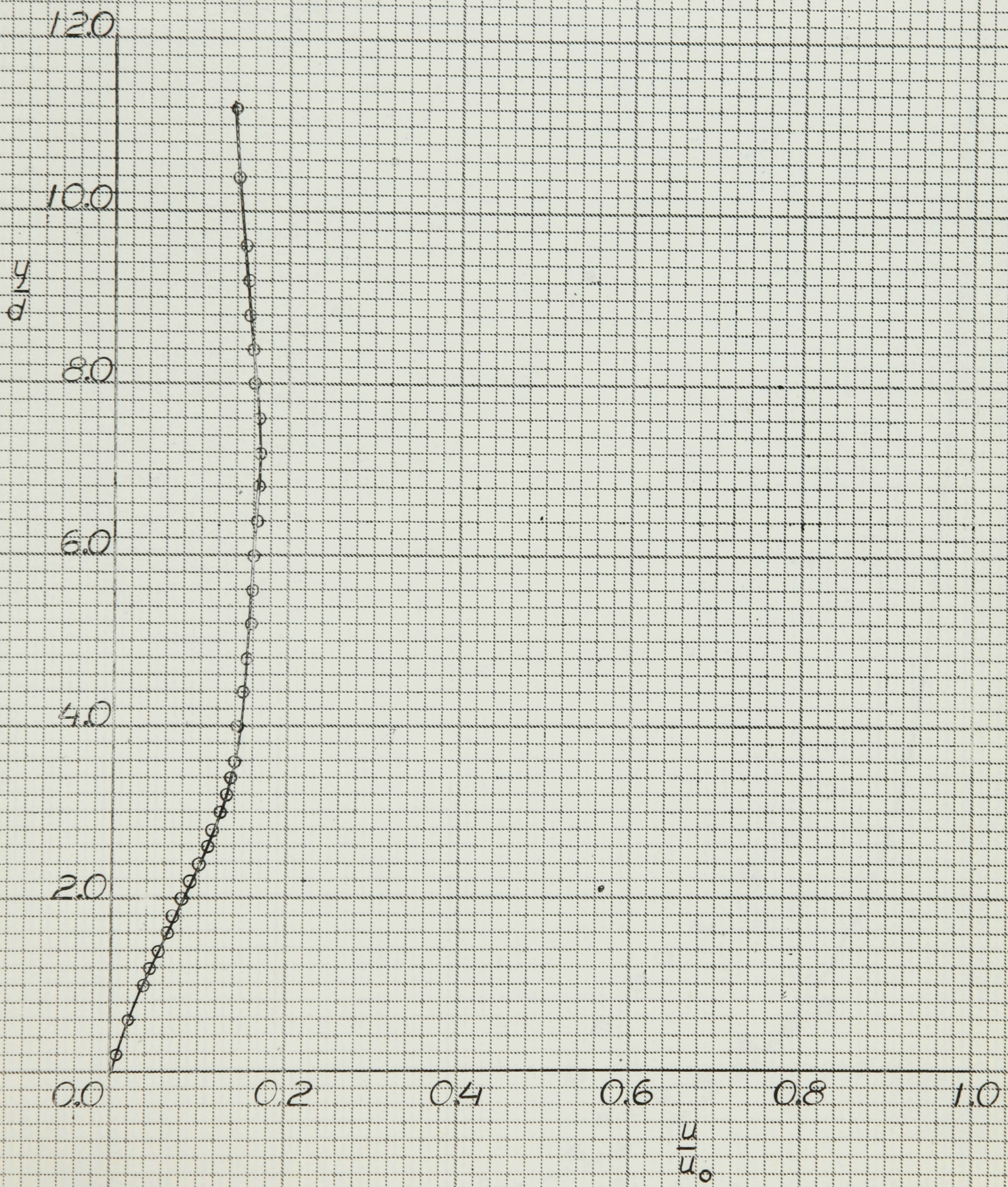


FIG. 23

MEAN VELOCITY PROFILE ON THE
 CIRCULAR CYLINDER FOR $\theta = 180^\circ$

$$Re = \left[\frac{(p_0 - p_\infty) b_e a}{\rho v^2} \right]^{\frac{1}{2}} = 5.5 \times 10^4$$

 $s/d = 1.5$

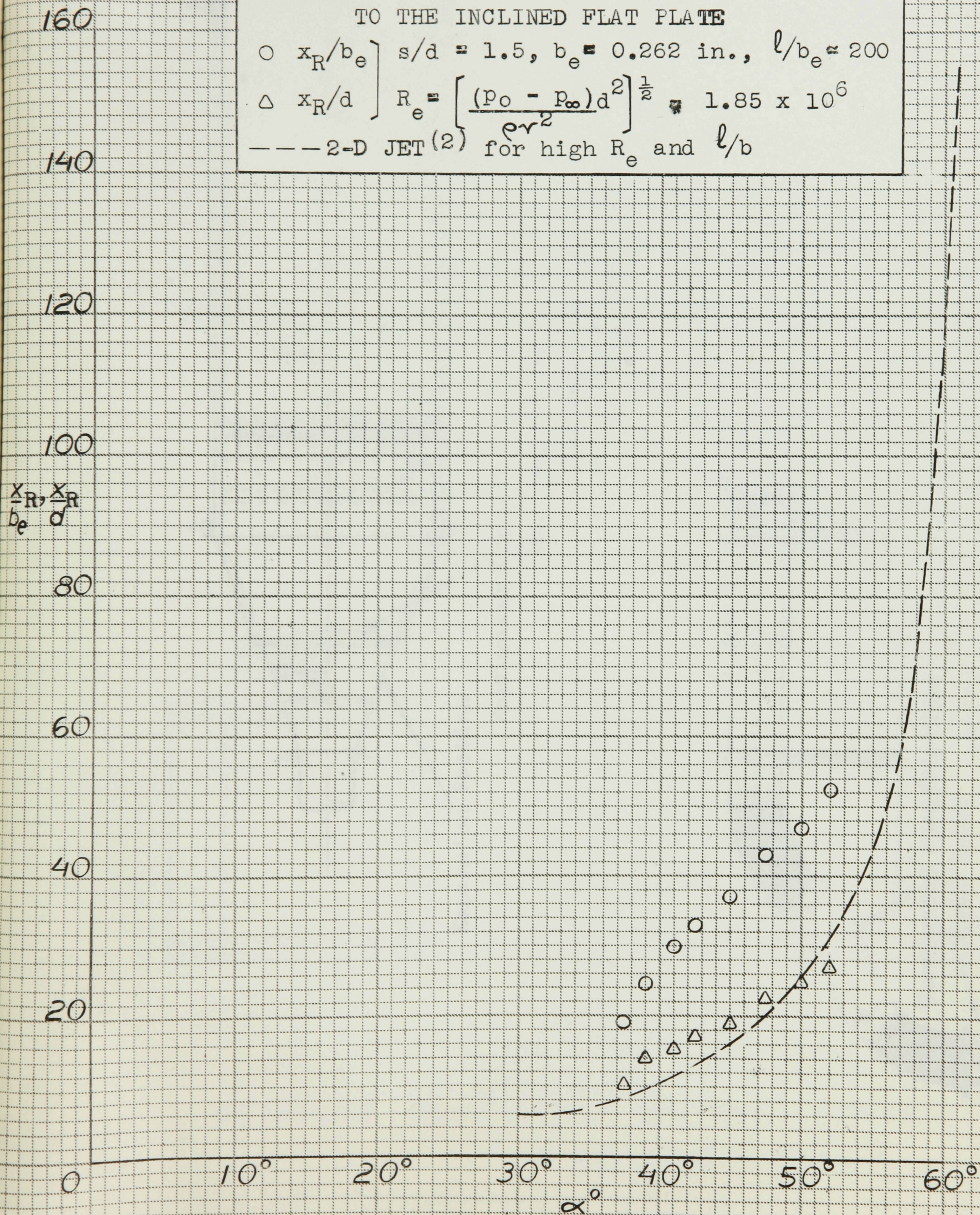


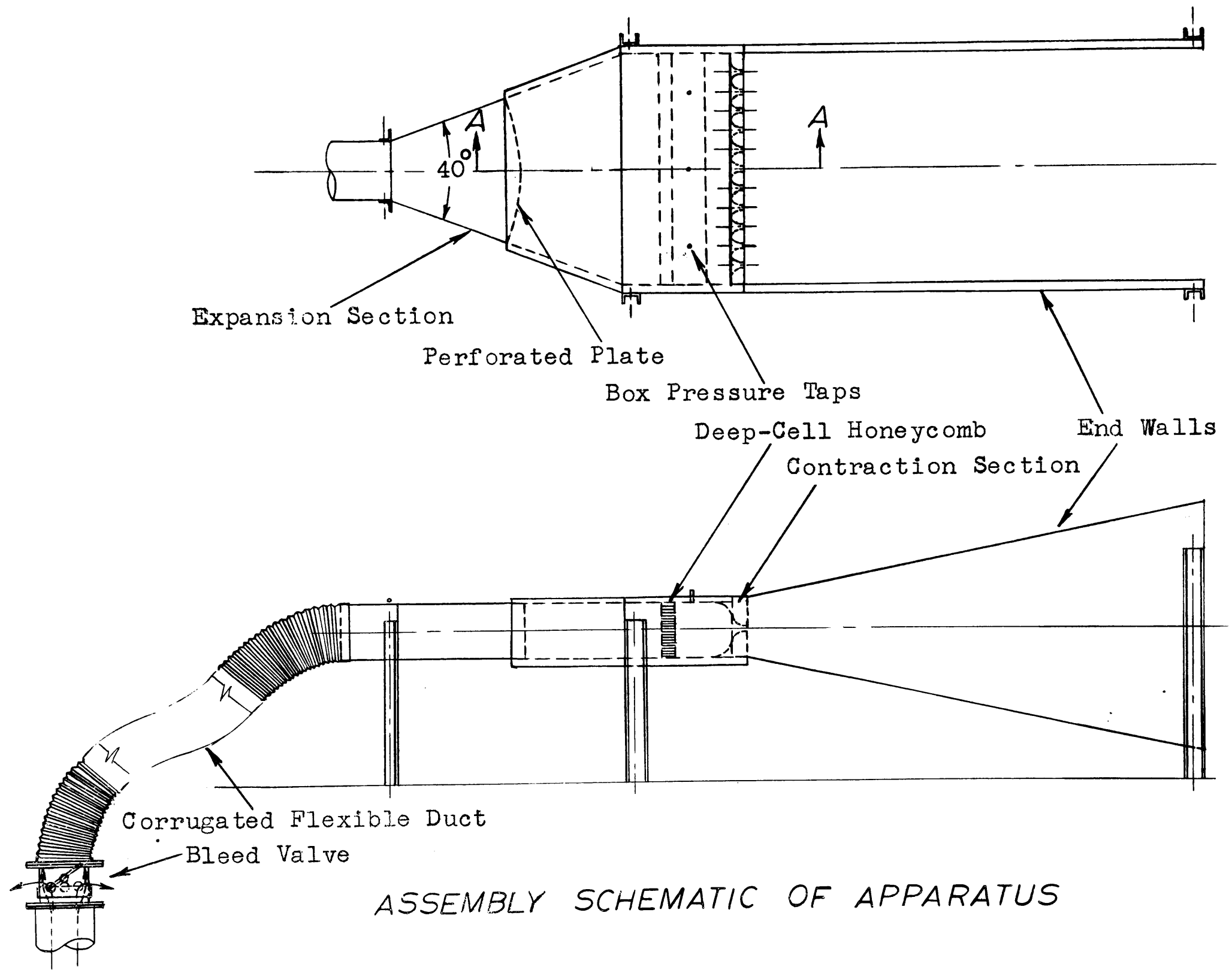
REATTACHMENT DISTANCE OF THE QUASI 2-D
TO THE INCLINED FLAT PLATE

○ x_R/b_e } $s/d = 1.5, b_e = 0.262 \text{ in.}, l/b_e = 200$

△ x_R/d } $R_e = \left[\frac{(p_0 - p_\infty)d^2}{\rho v^2} \right]^{1/2} = 1.85 \times 10^6$

--- 2-D JET (2) for high R_e and l/b





Expansion Section

Perforated Plate

Box Pressure Taps

Deep-Cell Honeycomb

End Walls

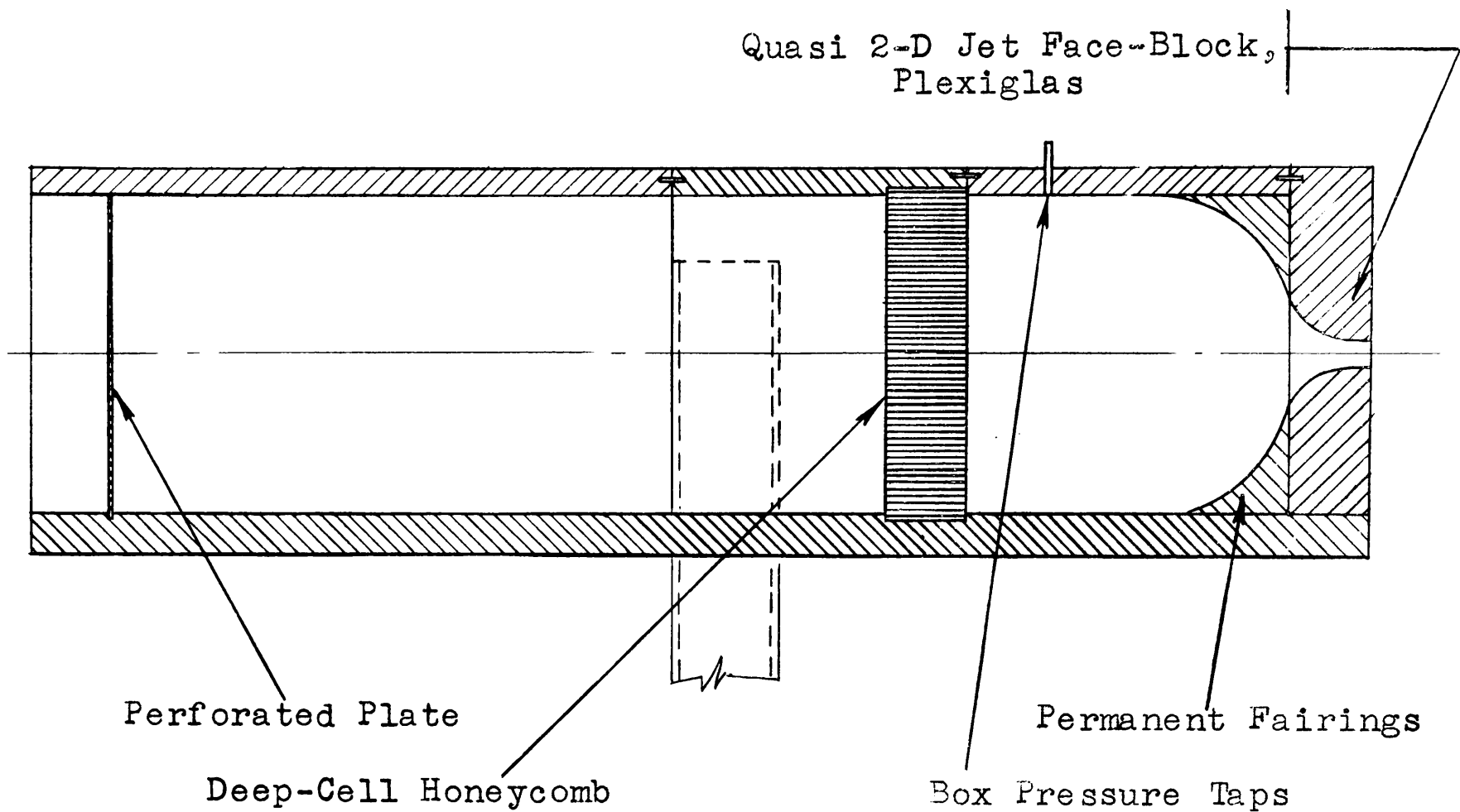
Contraction Section

Corrugated Flexible Duct

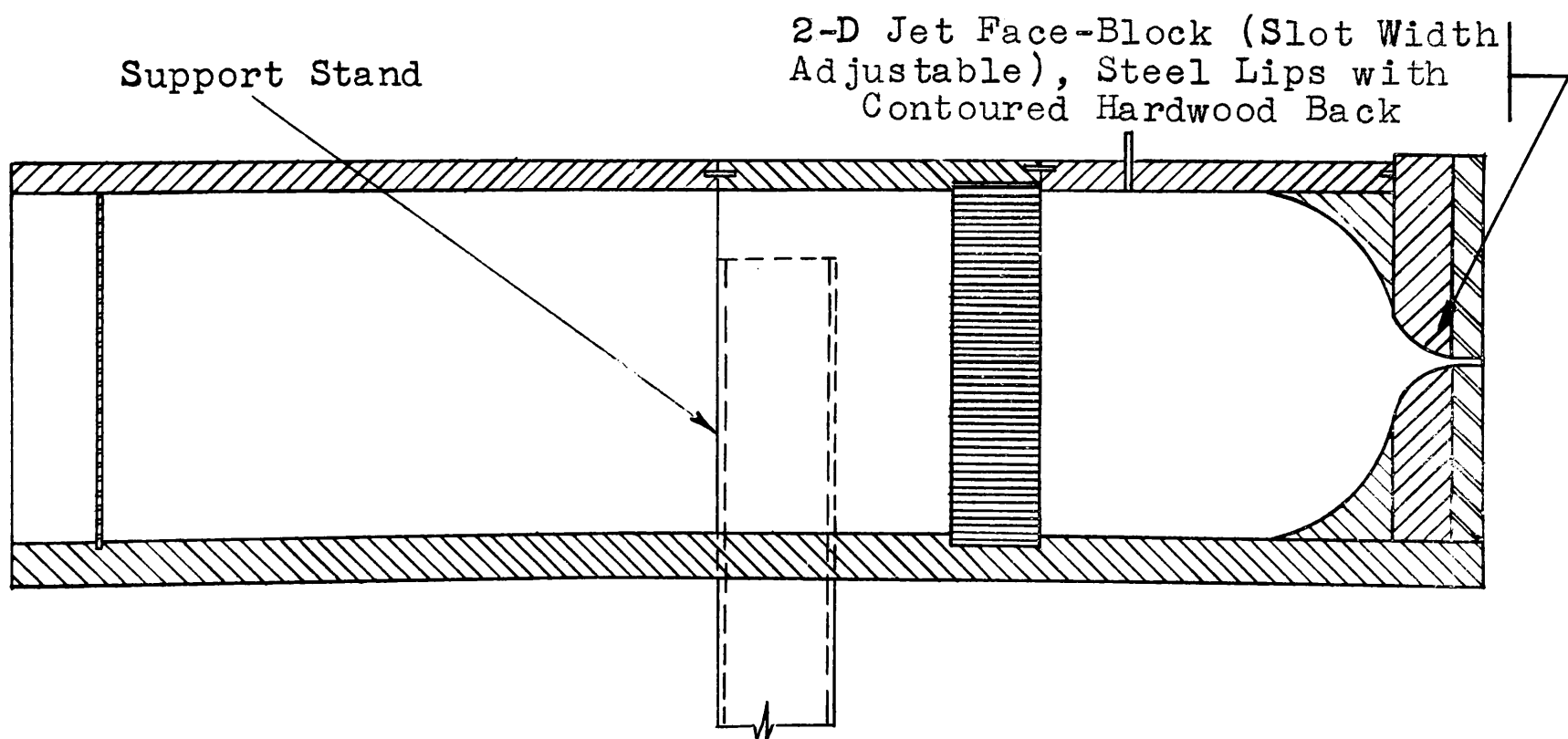
Bleed Valve

ASSEMBLY SCHEMATIC OF APPARATUS

FIG.25



SECTION A - A



DETAILED SCHEMATIC OF THE CONTRACTION

SECTION

FIG. 26

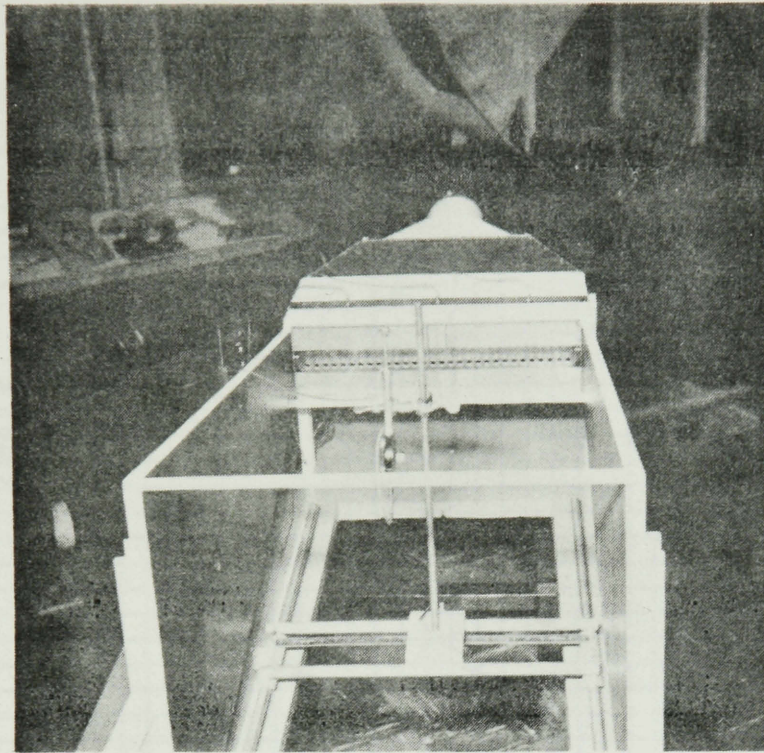


FIG. 27

GENERAL VIEW OF THE APPARATUS

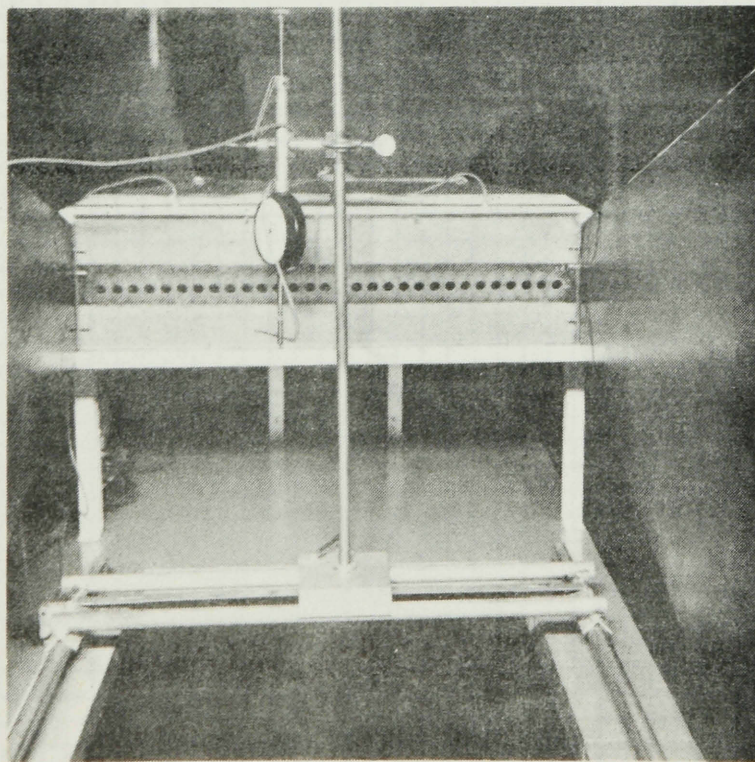


FIG. 28

THE SERIES OF HOLES IN LINE WITH $\frac{s}{d} = 1.5$ AND
THE TRAVERSING GEAR WITH THE PITOT
TUBE YAWED TO SHOW THE DIAL GAUGE

CALIBRATION OF THE ROUND PITOT
TUBE IN YAW AND PITCH

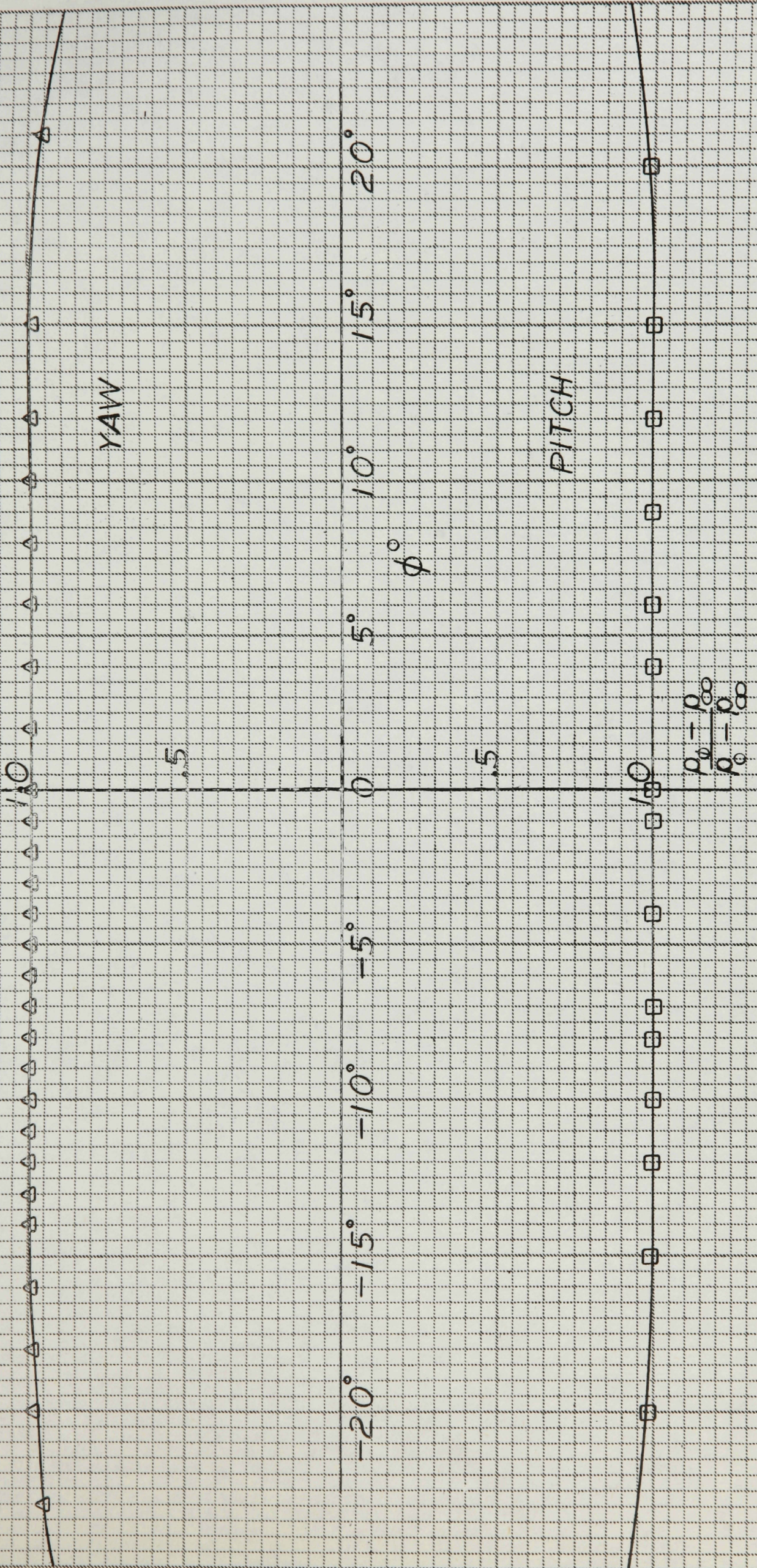


FIG. 30

